General Disclaimer

One or more of the Following Statements may affect this Document

- This document has been reproduced from the best copy furnished by the organizational source. It is being released in the interest of making available as much information as possible.

- This document may contain data, which exceeds the sheet parameters. It was furnished in this condition by the organizational source and is the best copy available.

- This document may contain tone-on-tone or color graphs, charts and/or pictures, which have been reproduced in black and white.

- This document is paginated as submitted by the original source.

- Portions of this document are not fully legible due to the historical nature of some of the material. However, it is the best reproduction available from the original submission.

DOE/NASA/0241-9
NASA CR- 168239

DEVELOP AND TEST FUEL CELL POWERED ON-SITE INTEGRATED TOTAL ENERGY SYSTEMS: PHASE III, FULL-SCALE POWER PLANT DEVELOPMENT

9TH QUARTERLY REPORT: FEBRUARY - APRIL, 1983

ENGELHARD INDUSTRIES DIVISION
ENGELHARD CORPORATION
EDISON, NJ 08818
H. Feigenbaum
A. Kaufman, Contract Manager
C. L. Wang
J. Werth
J. A. Whelan

REPORT DATE: July 5, 1983

PREPARED FOR
NATIONAL AERONAUTICS AND SPACE ADMINISTRATION
LEWIS RESEARCH CENTER
UNDER CONTRACT DEN3-241

for
U.S. DEPARTMENT OF ENERGY
ENERGY TECHNOLOGY
DIVISION OF FOSSIL FUEL UTILIZATION
UNDER INTERAGENCY AGREEMENT DE-AI-01-80ET17088

(NASA-CR-168239) DEVELOP AND TEST FUEL CELL POWERED ON-SITE INTEGRATED TOTAL ENERGY SYSTEM Quarterly Report, Feb. - Apr. 1983 (Engelhard Industries, Inc.) 42 p
HC A03/MF A01
CSCL 10A G3/44

N84-13673
Unclas
42987

SECTION I. INTRODUCTION

Engelhard's objective under the present contract is to contribute substantially to the national fuel conservation program by developing a commercially viable and cost-effective phosphoric acid fuel cell powered on-site integrated energy system (OS/IES). The fuel cell offers energy efficiencies in the neighborhood of 40% of the lower heating value of available fuels in the form of electrical energy. By utilizing the thermal energy generated for heating, ventilating, and air-conditioning (HVAC), a fuel cell OS/IES could provide total energy efficiencies in the neighborhood of 80%. Also, the Engelhard fuel cell OS/IES, which is the objective of the present program, offers the important incentive of replacing imported oil with domestically produced fuel.

Engelhard has successfully completed the first two phases of a five-phase program. The next three phases entail an integration of the fuel cell system into a total energy system for multi-family residential and commercial buildings. The mandate of Phase III is to develop a full-scale 50kW breadboard power plant module and to identify a suitable type of application site. Toward this end, an objective in Phase III is to complete the integration and testing of the 5kW system whose components were developed during Phase II. In addition to the development and testing of this sub-scale system, scale-up activities are to be implemented as a total effort for Phase III. Throughout this design and engineering program, continuing technology development activity will be maintained to assure that the performance, reliability, and cost objectives are attained.

SECTION II. TECHNICAL PROGRESS SUMMARY

TASK I - 5kW POWER SYSTEM DEVELOPMENT

The objective of this task is to complete integration of 5kW components and sub-systems developed during Phase II.

Modifications to the 5kW system's control system are in progress, although not all of the required electronic components have been received. Upon completion, this rework will establish capability for fully automatic system operation over the entire range of power levels.

TASK II - ON-SITE SYSTEM APPLICATION ANALYSIS

The purpose of this task is to develop an application model for on-site integrated energy systems. The model considers fuel availability, costs, building types and sizes, power distribution requirements (electrical and thermal), waste heat utilization potential, types of ownership of the OS/IES, and grid connection vs. stand-alone operation. The work of this task is being carried out under subcontract by Arthur D. Little, Inc. (ADL).

The basic structure of the economic analysis has been to compute the internal rate of return to the building owner of various fuel cell-based OS/IES systems versus a conventionally-powered system. The four building types selected are:

SECTION II. - CONTINUED

- Hospital
- Retail Store
- Apartment Building
- Office Building

These were analyzed over four different electric rate structures representing four combinations of the basic conditions principally affecting charges for electricity:

- High load growth rate
- Low load growth rate
- High oil/gas
- Low oil/gas

Additional variables included in the analysis were climate (Houston, Washington, Chicago), use of centrifugal chillers or absorption chillers for air-conditioning, and the option of thermal storage for thermal-load levelling.

A draft final report on this effort has been received from ADL. Results for the various cases have been presented using internal rate of return and incremental internal rate of return with increasing fuel cell power system capacity as figures of merit. These and other factors have been used in developing an approach for market size estimation.

A meeting between ADL and Engelhard was held on April 4, 1983 to discuss modifications to the draft report. The issues resolved at the meeting concerned the sizes and numbers of buildings that are attractive candidates for fuel cell OS/IES, the electricity sell-back assumptions, and the economics surrounding the use of absorption chillers. Action items were agreed upon to allow ADL to proceed with finalization of the report.

SECTION II. - CONTINUED

TASK III - ON-SITE SYSTEM DEVELOPMENT

This task forms the core of the Phase III Contract. Work under this task will result in the breadboard design of a system for an on-site application. The power plant will be designed for a rated output of 50kW (electrical) or some multiple thereof. The fuel processor and power conditioner will each be 50kW units, while the 50kW fuel cell will comprise two 25kW stacks. This task is accordingly broken down into four sub-tasks as follows:

3.1 Large Stack Development
3.2 Large Fuel Processor Development
3.3 Overall System Analysis
3.4 Overall System Design and Development

A large part of Sub-Task 3.3 was carried out by Physical Sciences, Inc. (PSI) under subcontract.

A. LARGE STACK DEVELOPMENT

The 24-cell, two-ft^2 (13" x 22") stack was constructed and put on test during February. It completed a 500-hour run on H_2/air reactants, operating in the temperature range of 350-385°F (177-197°C) and in the current density range of 50-150 ASF. As seen in Figure 1, the stack voltage was steady throughout the test at 15 volts at 150 ASF (161 mA/cm^2), yielding a power of about 4kW (Figure 2). The average cell voltage was 0.625V at the above current density (Figure 3).

The distribution of reactant gases in this stack was accomplished by utilizing in-situ distribution tubes, two of which were placed horizontally across each inlet manifold.

SECTION II. - CONTINUED

A new hydrogen manifold seal configuration was evaluated during this test. A schematic description of the sealing interface is shown in Figure 4. The manifold is fabricated with a 70° "wrap-around" corner which applies pressure on the Viton sealing gasket (upon manifold compression). Part of the gasket material flows around the 70° corner resulting in additional sealing area. This configuration resulted in undetectable hydrogen leaks (as analyzed using a detector probe) throughout the operation of the stack.

Another study carried out during this stack test involved sealing the interface between the metallic cooling plates and the carbon termination plates. Utilization of a Viton gasket at this interface was examined for the purpose of eliminating reactant gas leakage without interfering with electrical conduction. This approach (which utilizes a groove milled in the termination plate to accept the gasket) appears promising in that hydrogen leakage at these interfaces was undetectable and through-plane conduction was not adversely affected.

A carbon plate wet-proofing process was utilized for the first time in this 24-cell stack test. The wet-proofing of the graphite termination and bipolar plates by impregnation with FEP-120 prevented significant acid take-up, which had occurred during the testing of previous stacks. It was also determined that the corrosion resistance of these carbon plates in phosphoric acid was significantly improved as a result of this treatment (see Task IV, below).

A simplified acid-management configuration was evaluated in this stack for the first time. This system operated successfully throughout the test, maintaining an average cell open-circuit voltage of 0.87V.

Testing of the 24-cell stack with metallic cooling plates continued during March. A comprehensive study of temperature

SECTION II. - CONTINUED

distribution throughout the stack was performed at a current density of 150 ASF (161 mA/cm^2) using H_2/air reactants. The air and hydrogen were preheated to 200°F (93°C) at the stack entrance. The tests were performed at two air flow rates: 2.5 x stoichiometric (40% utilization) and 5 x stoichiometric (20% utilization). (The temperature profiles are shown in Figures 5, 6, 7 and 8.)

Figures 5 and 6 show the temperature profiles of two cells in a four-cell sub-stack (four-cell units between cooling plates). One of them is adjacent to a cooling plate (Cell No. 12), and the other is mid-way between cooling plates (Cell No. 10). These profiles were measured with a high air flow rate (5 x stoichiometric). It can be seen that the coolest region in each cell is at the air entrance (which was preheated only to 200°F). The range of temperatures in Cell No. 10 was 20°F (11°C) while the temperature range in Cell No. 12, which is adjacent to a cooling plate, was 15°F (8°C).

When the air flow rate was decreased to 2.5 x stoichiometric, the temperature range from the coolest to the hottest region in each cell was reduced to only 10°F (5.5°C); see Figures 7 and 8. For sub-stacks removed from the top and bottom ends of the stack the maximum temperature difference from the coolest region of the coolest cell to the hottest region of the hottest cell was only 12°F (7°C). This suggest that (with bipolar plates utilizing graphite elements, at least) the number of cells between cooling plates can be increased to five, and perhaps more.

The effect of air flow rate on cell performance in the 24-cell stack was also studied. Figure 9 shows the voltage-current curves for the stack at 375°F (191°C) and various air flow rates (2, 2.5, 3, 3.5, and 5 x stoichiometric). As expected, the average cell performance is higher at higher flow rates; however, the differences in cell voltage are rather small. For example, at 150 ASF and 5 x stoichiometric air flow, the average cell performance is 15 mV higher than in the case of 2.5 x stoichiometric air flow.

SECTION II. - CONTINUED

At the beginning of April, five non-metallic cooling plates were assembled into the 24-cell stack, replacing the metallic cooling plates originally used. Operation was trouble-free throughout the month. Cooling plate interfacial IR-losses were insignificant.

Temperature distribution profiles of all 24 cells in the stack were measured at 150 ASF with an air flow rate of 2.5 x stoichiometric. The profiles (excluding those of cells in the outboard sub-stacks), are illustrated in Figure 10. These show a maximum ΔT within any cell of 5°C and a maximum centerline ΔT among cells in the same sub-stack of 6°C. Although these measurements show a high degree of temperature uniformity, further thermal data acquisition is planned for May. The coolant manifolds will be reworked to allow accurate measurements of coolant inlet and outlet temperatures.

Construction activity for the 25kW stack is currently in abeyance.

B. LARGE FUEL PROCESSOR DEVELOPMENT

The burner and heat exchanger assembly of the 50kW fuel processing sub-system was tested with water flowing in the heat exchanger coils. This assembly is shown schematically in Figure 11. The function of the upper heat exchanger coil is to transfer heat to the HVAC sub-system, while that of the lower coil is to preheat the CH_3OH-H_2O reactants to the reformer inlet temeprature.

The burner's heat generation rate was approximately 120,000 Btu/hr (~2 gal/hr of methanol). About 70% of this heat was transferred to the two heat exchanger coils, while the sensible heat in the combustion gas exhaust accounted for an additional 21%. The balance (about 11,000 Btu/hr) is attributed to heat loss through

the wall of the assembly. The overall heat-transfer coefficient at the CH_3OH-H_2O preheater coil was calculated to be approximately 5.7 Btu/hr-ft^2-°F. The equipment performance in this test was judged to be satisfactory, and no problems or unanticipated results were encountered.

Further test and evaluation activity for the 50kW fuel processing sub-system is currently in abeyance.

C. OVERALL SYSTEM ANALYSIS

The Physical Sciences Inc. subcontract has been completed. Final reports involving the off-design and transient analysis portions of the work have been received. The corresponding computer modules have been integrated into the overall fuel cell system program, and trial runs have been executed to lay the groundwork for parametric optimization studies.

D. OVERALL SYSTEM DESIGN AND DEVELOPMENT

A review of The Trane Co. subcontract was held at Engelhard on March 8, 1983 to discuss the heat recovery sub-system and the overall system integration. The parameters studied by Trane included the effects of fuel cell capacity, fuel cell cost, type of chiller, thermal storage, type of building, location, electric rate structure, and taxes on the dollar savings of on-site integrated energy fuel cell systems. The main conclusion of that part of the Trane study is that such systems are economically attractive in buildings with relatively high ratios of thermal to electrical load, such as hospitals and apartment buildings; in areas with medium or high electric rates; and for

fuel cell systems where the installed fuel cell system cost is relatively low. However, the greater the cost of electricity, the greater the allowable installed cost of the fuel cell system.

Trane also analyzed an Engelhard-proposed concept relating to the heat recovery sub-system. This analysis and the results are presented in the Appendix.

The economic effects resulting from fuel cell thermal output in various proportions of "high-quality" (~175°C) heat and "medium-quality" (~93°C) heat were studied by Trane. The results, in terms of net present value (NPV), internal rate of return (IRR), and simple payback (SPB), are presented in Table I for a hospital using electric chillers, double-effect absorption chillers, and hot water storage. Table I shows that as the percentage of high-quality heat (i.e., that suitable for double-effect absorption chillers) shrinks to 50% and below, the internal rate of return remains high, but the net present value starts to shrink. (This reflects a loss of the cost savings opportunity presented by absorption chillers, which reduce the electrical load of the building.)

Another situation analyzed by Trane concerned hypothetical cases where sell-back to the utility would not be permitted, so that the fuel cell output would have to be lowered during off-peak hours. In the case of the hospital, this would lower the internal rate of return from 33.4% to 31.6%, not enough to seriously degrade the economics of the concept. In the case of the apartment complex, however, the IRR would fall from 29.5% to 18.7%, a drop large enough to have a potentially adverse effect on the future prospects of fuel cell systems for apartment complexes.

SECTION II. - CONTINUED

TASK IV - STACK SUPPORT

The purpose of this task, which will continue throughout the contract, is to investigate new materials and component concepts by experimentation and the use of small-stack trials. The criteria for choosing activities under this task are the prospects for improved performance, reduced cost, or improved reliability. Improvements in and performances of electrocatalysts, though generated under Engelhard-sponsored Task VI, will be reported under Task IV.

A. PERFORMANCE OPTIMIZATION

CATALYSTS

The electrocatalyst development effort continued to focus on improved cathode performance during the reporting period. A new formulation (E-7) is exhibiting high performance in the early stages of evaluation. The longest single-cell test time accumulated to date is about 1000 hours.

Figures 12 and 13 illustrate early voltage *vs.* current relationships for cathodes of this type. The corresponding steady-load histories for these cells to date are shown in Figures 14 and 15. Evaluation of the E-7 catalyst series will continue.

Depending on electrode fabrication procedures, the Pt surface-area of electrodes determined by the electrochemical hydrogen adsorption technique can vary significantly due to incomplete catalyst wetting. Figure 16 shows the voltammograms of two electrodes prepared using the same developmental catalyst (E-7). The Pt surface-area values obtained for these two electrodes were 106 m^2/gm Pt and 58 m^2/gm Pt. The low Pt surface-area for one electrode is attributed

to incomplete wetting of the carbon support. This contention is supported by the low double-layer charging current evident in Figure 16 (note base-line current at about 0.4V vs. RHE). Since the carbon support surface-area is the same for the two electrodes, the double-layer charging current should be the same if both electrodes were fully wetted.

Figure 17 shows a correlation between the double-layer charging current and the Pt surface-area for various electrode samples fabricated from this same catalyst. This correlation can be utilized to determine the degree of wetting of fuel cell electrodes and thereby avoid anomalously low values caused by incomplete wetting.

B. COST REDUCTION

BIPOLAR PLATES

An alternative graphite material, type 940G, is being examined in comparison to the HLM type for use as bipolar plate elements. Advantages of the 940G material include lower cost and lower corrosion rate.

Electrical tests of 10.7" x 14" ABA-type bipolar plate samples utilizing 940G graphite elements yielded entirely satisfactory results (see Appendix). Permeability tests were also conducted for bipolar plates fabricated from 940G elements. The details are presented in the Appendix. It was found that permeability rates were at least as low with 940G plates as with well-performing HLM plates, indicating that 940G remains an attractive bipolar plate element candidate.

SECTION II. - CONTINUED

C. RELIABILITY

NON-METALLIC COOLING PLATES

Several procedures involved in the fabrication of non-metallic cooling plates were worked out. These are described in the Appendix.

Seven non-metallic cooling plates were assembled for use in the 24-cell, two-ft^2 stack. One of the plates broke during assembly. The plates were tested, after assembly, for electrical resistance and coolant leaks. The voltage drops were less than 3 millivolts at rated current density (150 A/ft^2). No leaks were observed when the coolant was pressurized to 3.5 atmospheres.

The performance of these cooling plates in the 24-cell stack is described above under Task III.

CARBON PAPER SUBSTRATE WETPROOFING

Teardown analysis studies of fuel cells tested for long periods (exceeding 5000 hours) have indicated that the carbon fiber paper electrode substrate tends to slowly lose strength. This results from a continuous shear action applied by the grooved carbon plate, which is compressively loaded against the carbon paper. A creep process tends to occur, and this serves to rupture some carbon fibers. Activity has recently been carried out with the objective of improving the shear strength of the carbon paper substrate. This would benefit by sustaining the reactant gas diffusion properties within this element.

SECTION II. - CONTINUED

A variety of treatment techniques for the carbon paper substrate were evaluated this month. A fixture for measuring the shear strength of the treated and untreated carbon paper was constructed (Figures 18 and 19) and adapted to an Instron Model TM tester.

Initial results indicated that a significant improvement of the shear strength can be achieved by treating the carbon paper substrate with mixtures of fluoropolymers. Figure 20 shows the curve obtained for an untreated carbon paper substrate. Rupture occurred when the shear force reached 7 lb. On the other hand, carbon paper treated with 30% FEP-120 (presently used in the 24-cell stack) ruptured at a force of 14 lb. (Figure 21). A further significant increase in the shear strength was obtained when the carbon paper was treated with 50% TFE-30 (Figure 22). However, the wet proofing characteristics of this carbon paper were not as good as those treated with 30% FEP-120.

The most attractive results were obtained with two fluorocarbon mixtures (Figures 23 and 24 and Tables II and III). These mixtures were: (1) 20% FEP-120, 50% TFE-30 and (ii) 25% FEP-120, 50% TFE-30. Optimization of the treatment technique will be pursued in order to obtain higher shear strength, low electrolyte uptake (wetproofing), and satisfactory porosity.

BIPOLAR PLATE WETPROOFING

HLM graphite bipolar plate elements of the type that were to be used in the 24-cell, two-ft^2 stack were wetproofed using FEP-120 fluorocarbon dispersion in order to diminish their uptake of acid. This treatment was found to be effective, and it also serves to reduce the rate of corrosion of the graphite material.

SECTION II. - CONTINUED

Figure 25 shows the corrosion current of HLM graphite samples with and without wetproofing treatment. It is seen that the corrosion rate (at 0.9V vs. RHE) is effectively reduced by almost two orders of magnitude as a result of wetproofing.

TASK V - FUEL PROCESSING SUPPORT

The intent of this task is to provide background data and information to support the design and construction of an optimized 50kW fuel processor under Task III. Most of the effort of this task was devoted to screening and longevity testing of catalysts for methanol/steam reforming. This task is now complete.

TASK VI - IMPROVED ELECTROCATALYSTS

Developmental electrocatalyst formulations are being prepared under Engelhard sponsorship. These are provided to the main program, and results are reported under Task IV.

SECTION III. CURRENT PROBLEMS

TASK I - 5kW POWER SYSTEM DEVELOPMENT

- Some electronic components for 5kW fuel cell control system modifications not yet in hand.

SECTION IV. WORK PLANNED

TASK I - 5kW POWER SYSTEM DEVELOPMENT

- Complete modifications of 5kW fuel cell control system.

TASK II - ON-SITE SYSTEM APPLICATION ANALYSIS

- Implement changes in Arthur D. Little subcontract final report.

TASK III - ON-SITE SYSTEM DEVELOPMENT

- Continue testing of non-metallic cooling plates in 24-cell, two-ft^2 stack.

TASK IV - STACK SUPPORT

- Continue evaluation of E-7 cathode catalyst.

SECTION V. FINANCIAL MANAGEMENT ANALYSIS

TASK I - 5kW POWER SYSTEM DEVELOPMENT

Activity resumed on the integrated system during April with control system modifications. The total spending to date on this task is about $13,000 over the revised budget.

TASK II - ON-SITE SYSTEM APPLICATION ANALYSIS

No billing was made on the Arthur D. Little subcontract during April. About $6000 remains from the budget for this task. This should be adequate to complete the final report.

TASK III - ON-SITE SYSTEM DEVELOPMENT

1. Large Stack Development

Minor expenses were incurred on this sub-task during April. These entailed test activity for the 24-cell stack.

2. Large Fuel Processor Development

Virtually no labor effort was expended on this sub-task during April. The small amount of spending (about $2000) resulted predominantly from late invoices for materials purchases.

3. Overall System Analysis

This sub-task has been completed.

ENGELHARD

TABLE I

ECONOMIC IMPACT OF QUALITY OF FUEL CELL THERMAL OUTPUT

FUEL CELL SYSTEM CAPACITY (kW)	WASTE HEAT AT: 175°C (Percent)	93°C (Percent)	ELECTRIC CHILLING (Tons)	ABS CHILLING (Tons)	NPV * $ X1000	IRR (%)	SPB (Years)
460	96	4	384	125	655	35.0	2.2
460	89	11	393	116	649	34.9	2.2
460	48	52	446	63	615	34.7	2.2
440 **	0	100	509	0	573	34.6	2.2

* @ 15% After-tax hurdle rate

** Maximum capacity allowing complete utilization of fuel cell thermal output.

TABLE II

SHEAR STRENGTH OF CARBON PAPER

Sample	Force to Failure (lb.)	Shear Strength (lb/sq.in.±%)
Untreated	6.8	77^{+8}_{-12}
30% FEP-120	14.1	160^{+7}_{-5}
20% FEP-120, 50% TFE-30	28.4	322^{+6}_{-5}
25% FEP-120, 50% TFE-30	29.5	335^{+9}_{-6}
50% TFE-30	25.6	291^{+5}_{-8}

TABLE III

SHEAR STRENGTH OF ACID-SOAKED CARBON PAPER

Sample	Force to Failure (lb.)	Shear Strength (lb/sq.in.±%)
30% FEP-120	12.3	142 ± 1
20% FEP-120, 50% TFE-30	27.5	314 ± 9
25% FEP-120, 50% TFE-30	28.5	324 ± 3

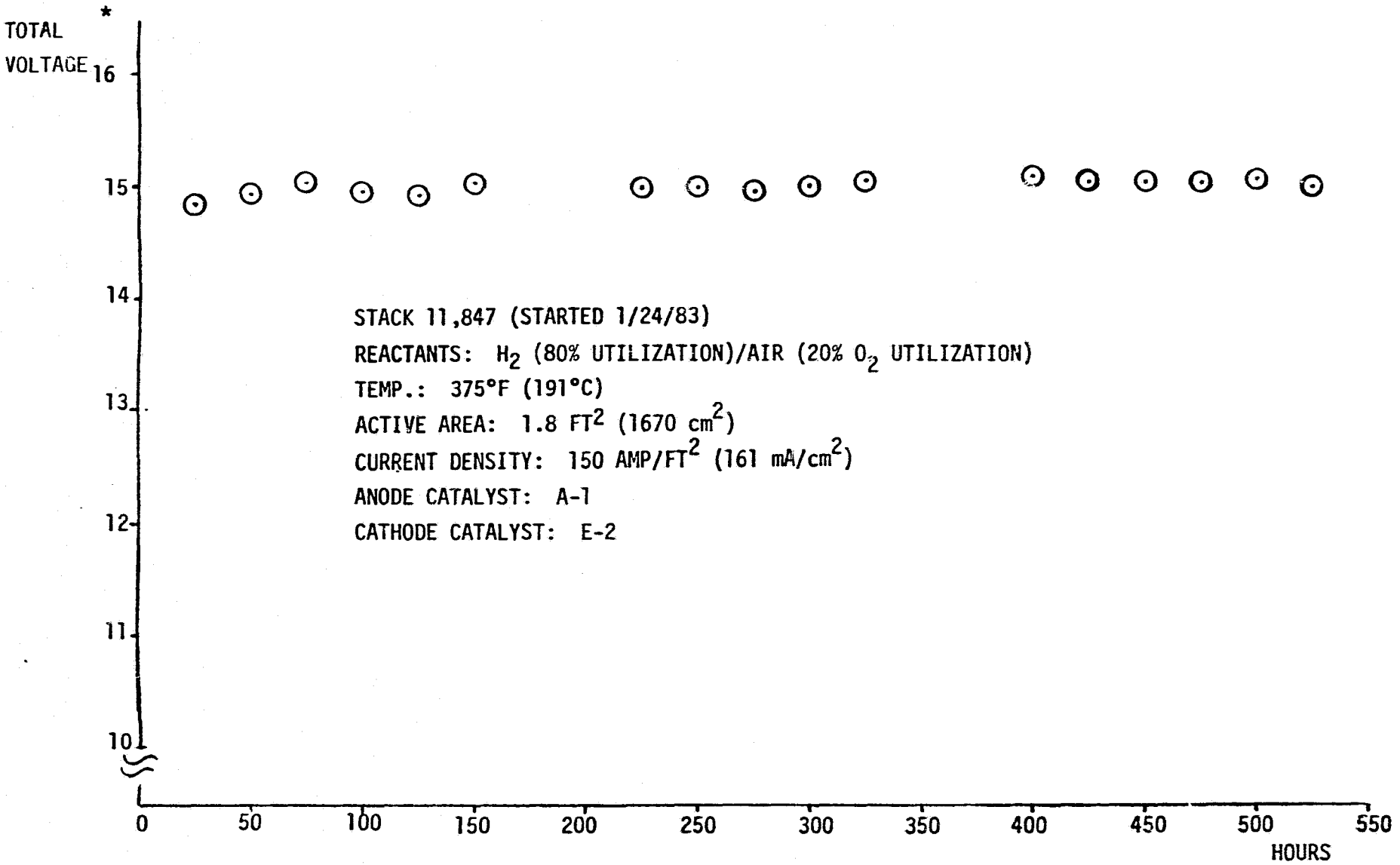

FIGURE 1 VOLTAGE STABILITY OF 24-CELL STACK (2 FT^2)

* SUM OF 24 INDIVIDUAL CELL VOLTAGES

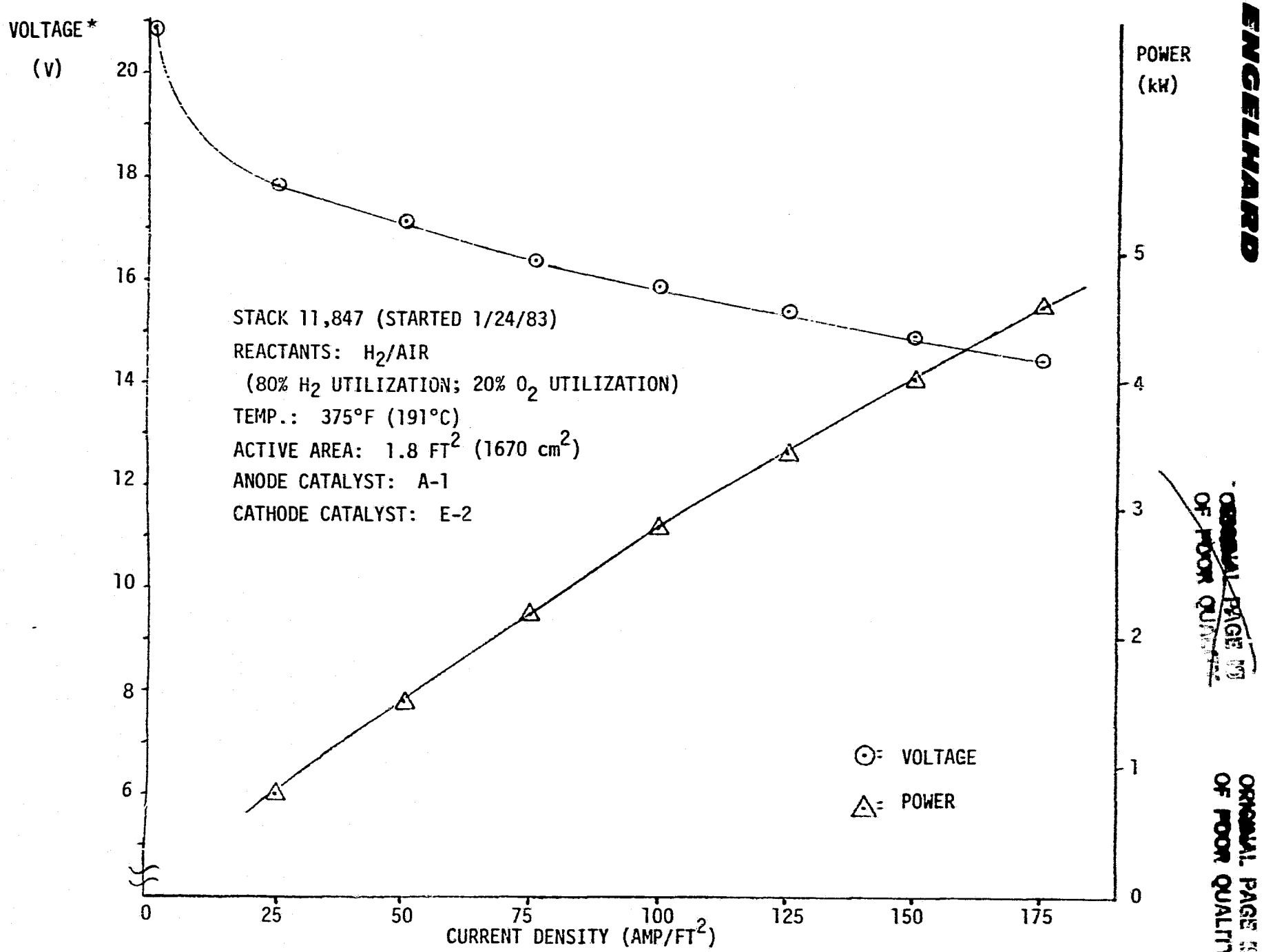

FIGURE 2 PERFORMANCE OF 24-CELL STACK (2 FT^2)

* SUM OF 24 INDIVIDUAL CELL VOLTAGES

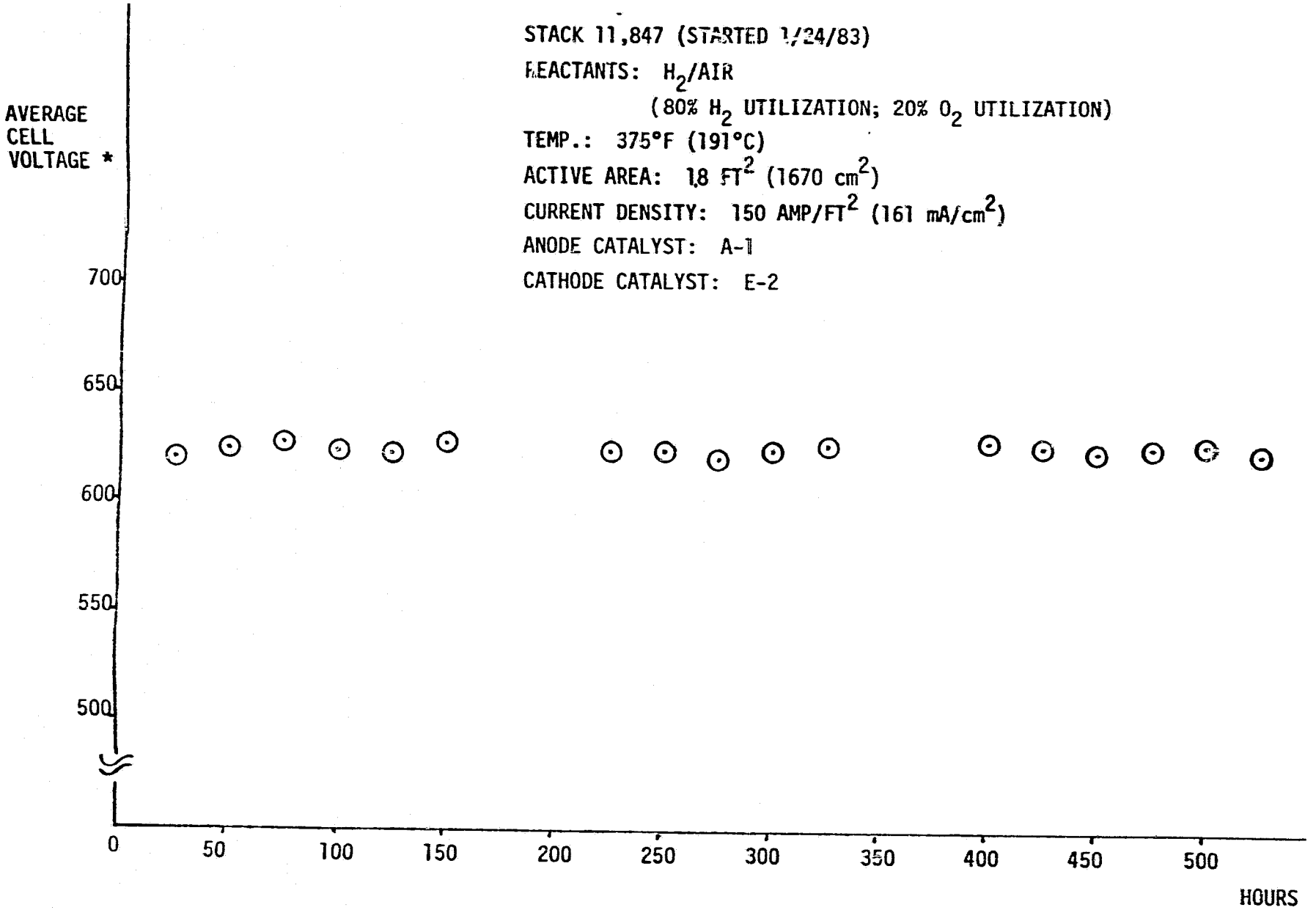

FIGURE 3 AVERAGE CELL VOLTAGE IN 24-CELL STACK

* AN AVERAGE OF 24 CELL VOLTAGES

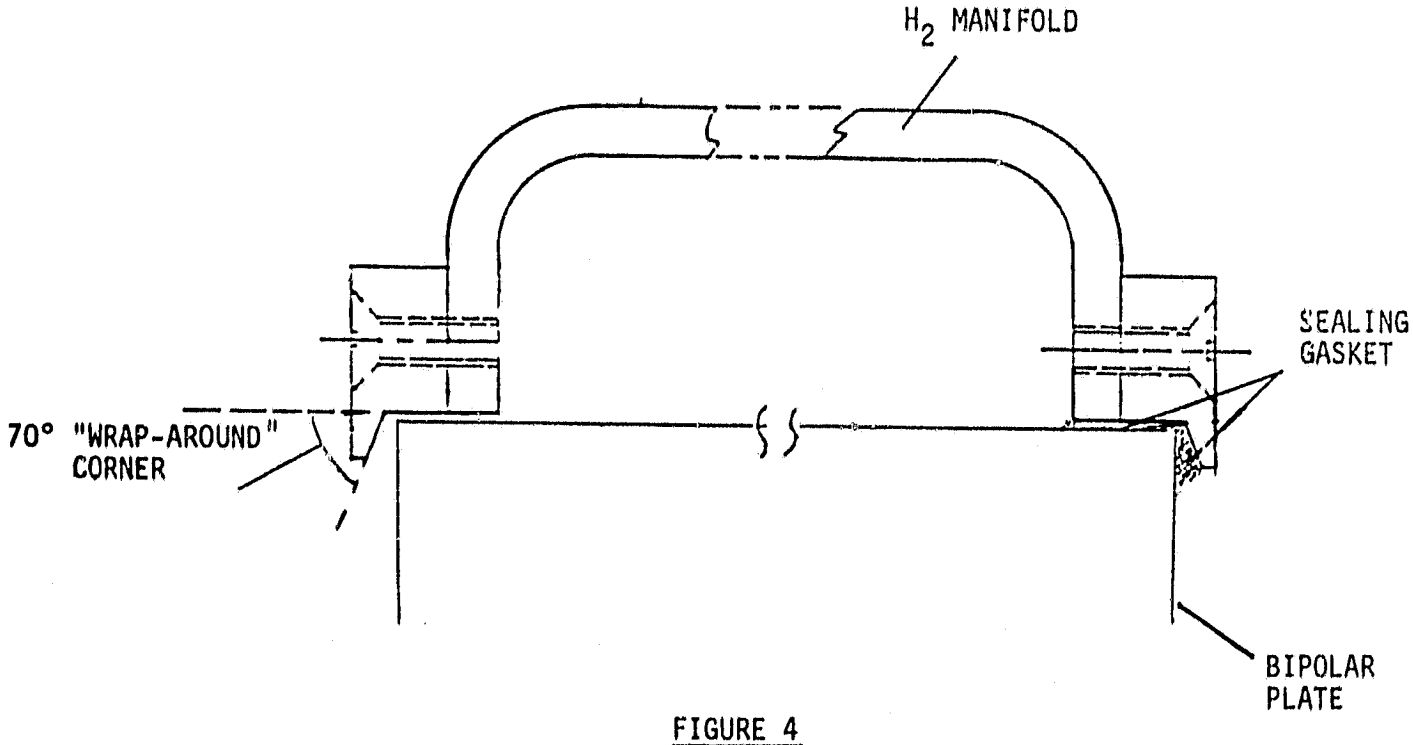

FIGURE 4

70° WRAP-AROUND HYDROGEN MANIFOLD CORNER SEAL

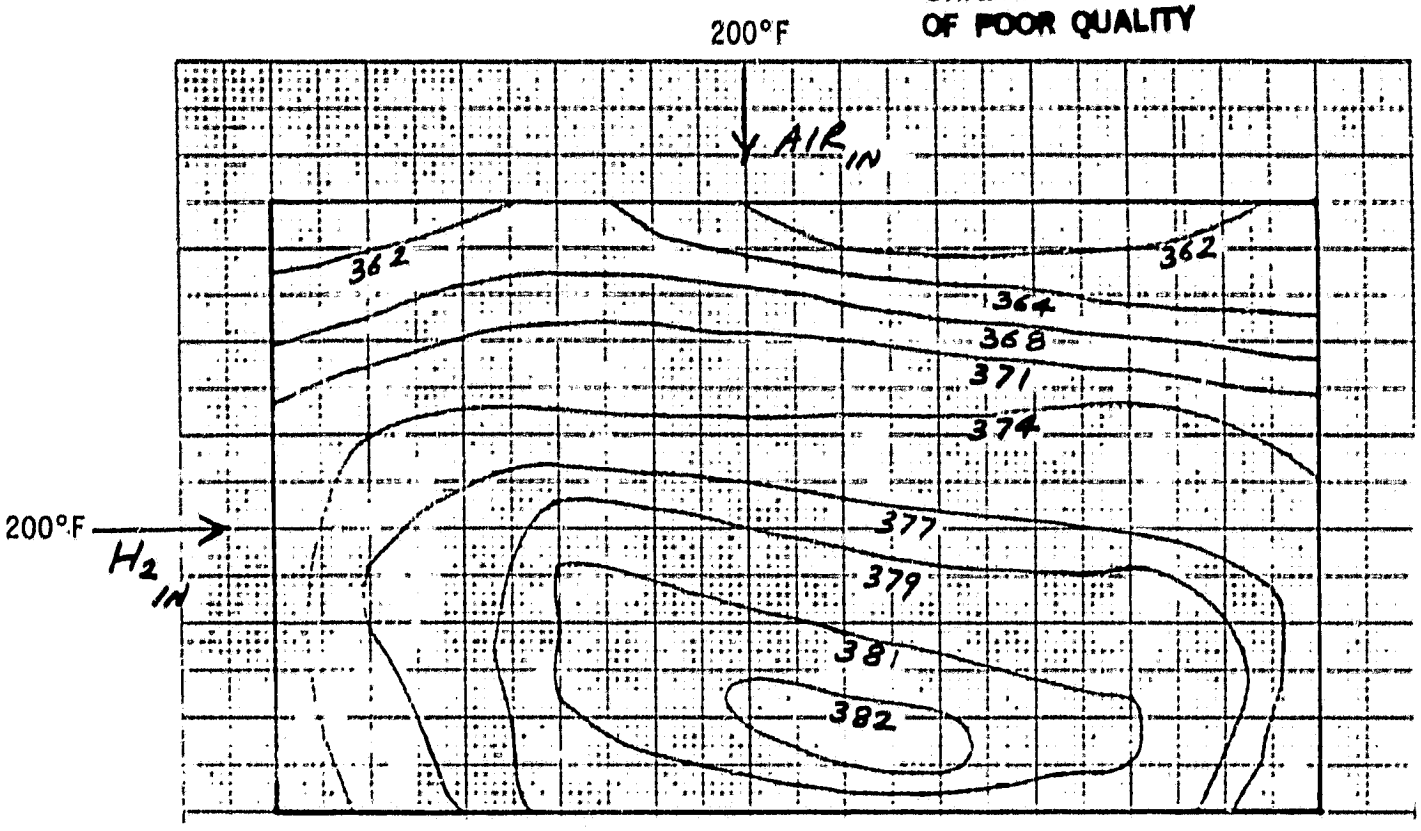

FIGURE 5 CELL TEMPERATURE PROFILE (°F) IN 24-CELL STACK WITH METALLIC COOLING PLATES

(MIDDLE OF SUB-STACK, CELL NO. 10; 5xSTOICH. AIR; 150 ASF; 200°F AIR PREHEAT TEMPERATURE)

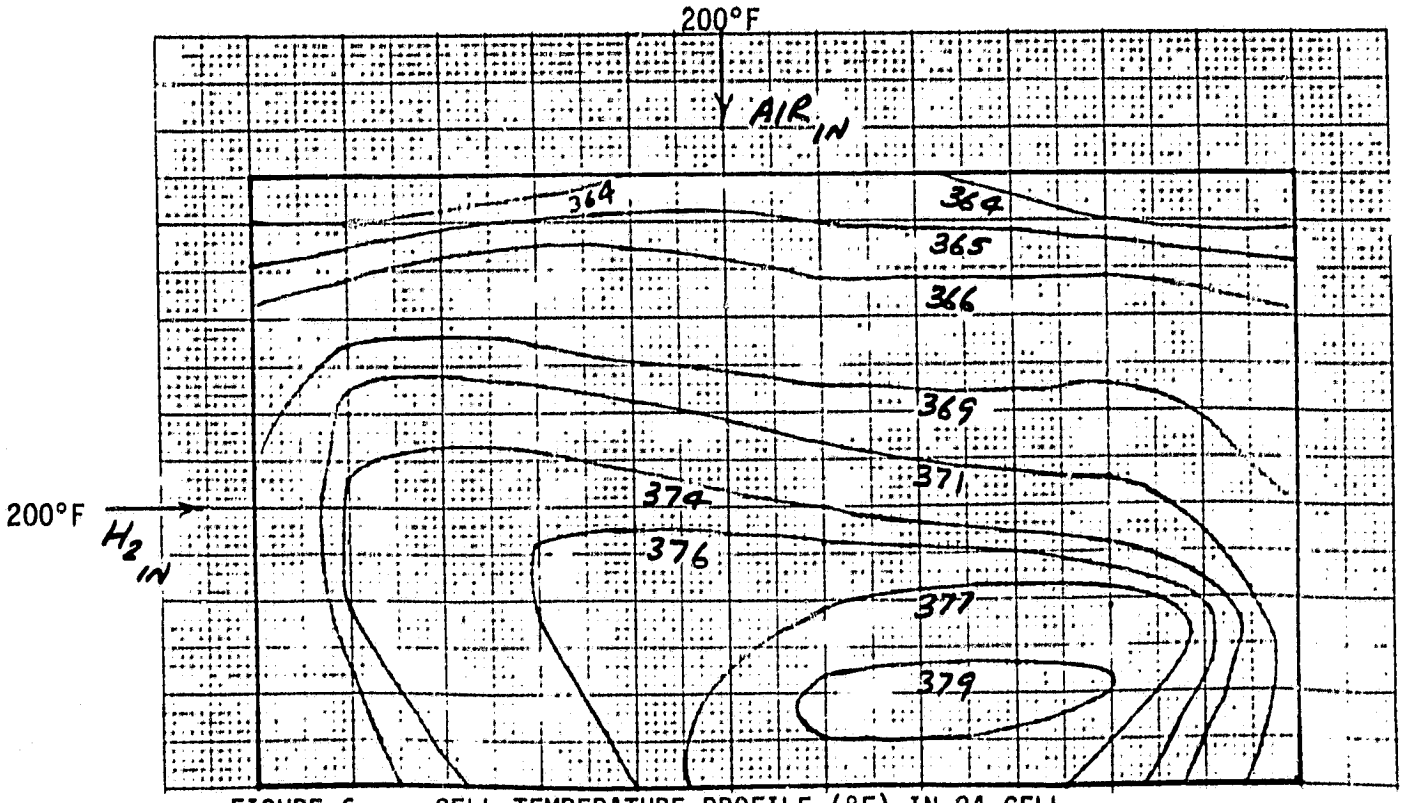

FIGURE 6 CELL TEMPERATURE PROFILE (°F) IN 24-CELL STACK WITH METALLIC COOLING PLATES

(ADJACENT TO COOLING PLATE, CELL NO. 12; 5xSTOICH. AIR; 150 ASF; 200°F AIR PREHEAT TEMPERATURE)

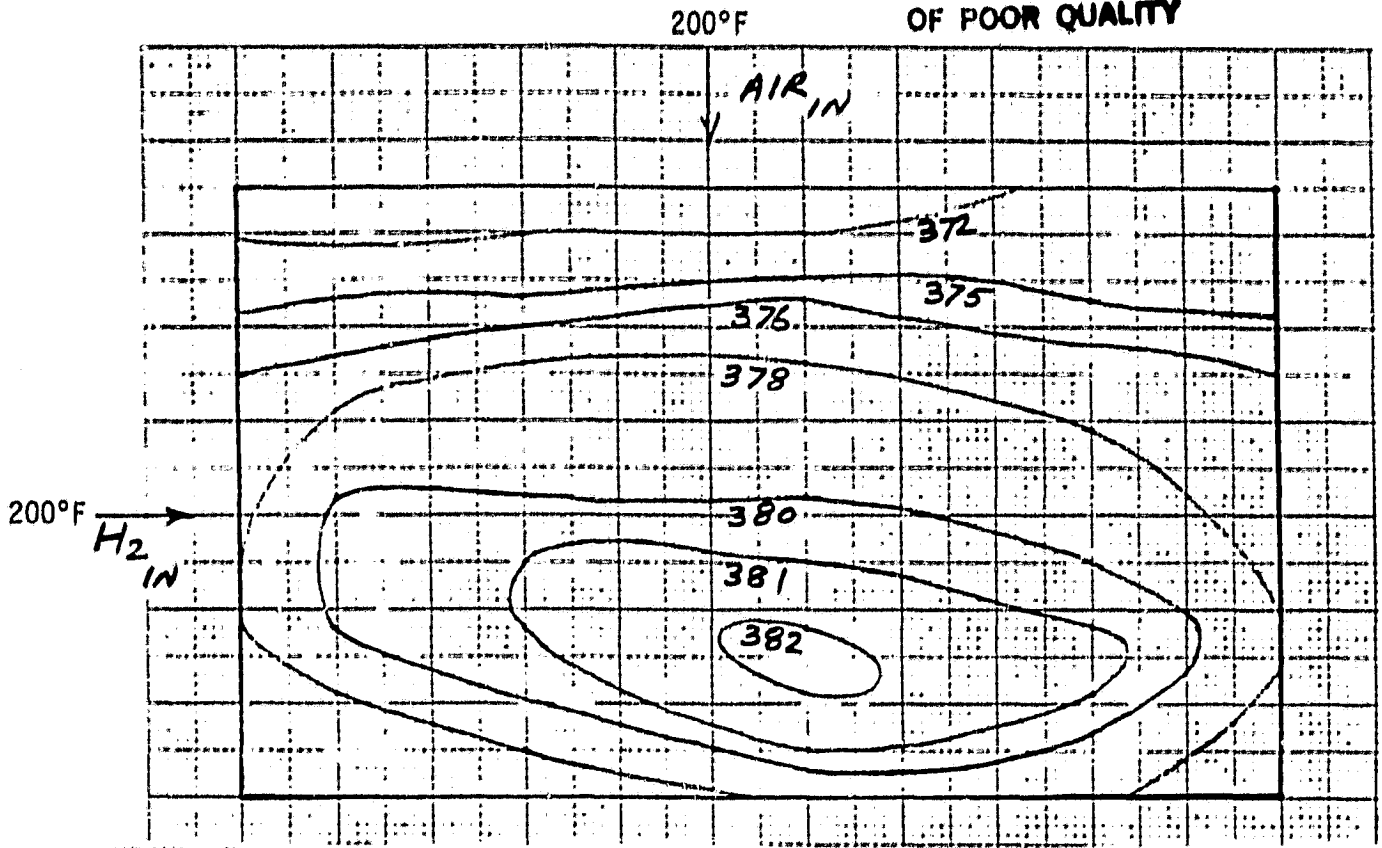

FIGURE 7 CELL TEMPERATURE PROFILE (°F) IN 24-CELL STACK WITH METALLIC COOLING PLATES

(MIDDLE OF SUB-STACK, CELL NO. 10; 2.5x STOICH. AIR; 150 ASF; 200°F AIR PREHEAT TEMPERATURE)

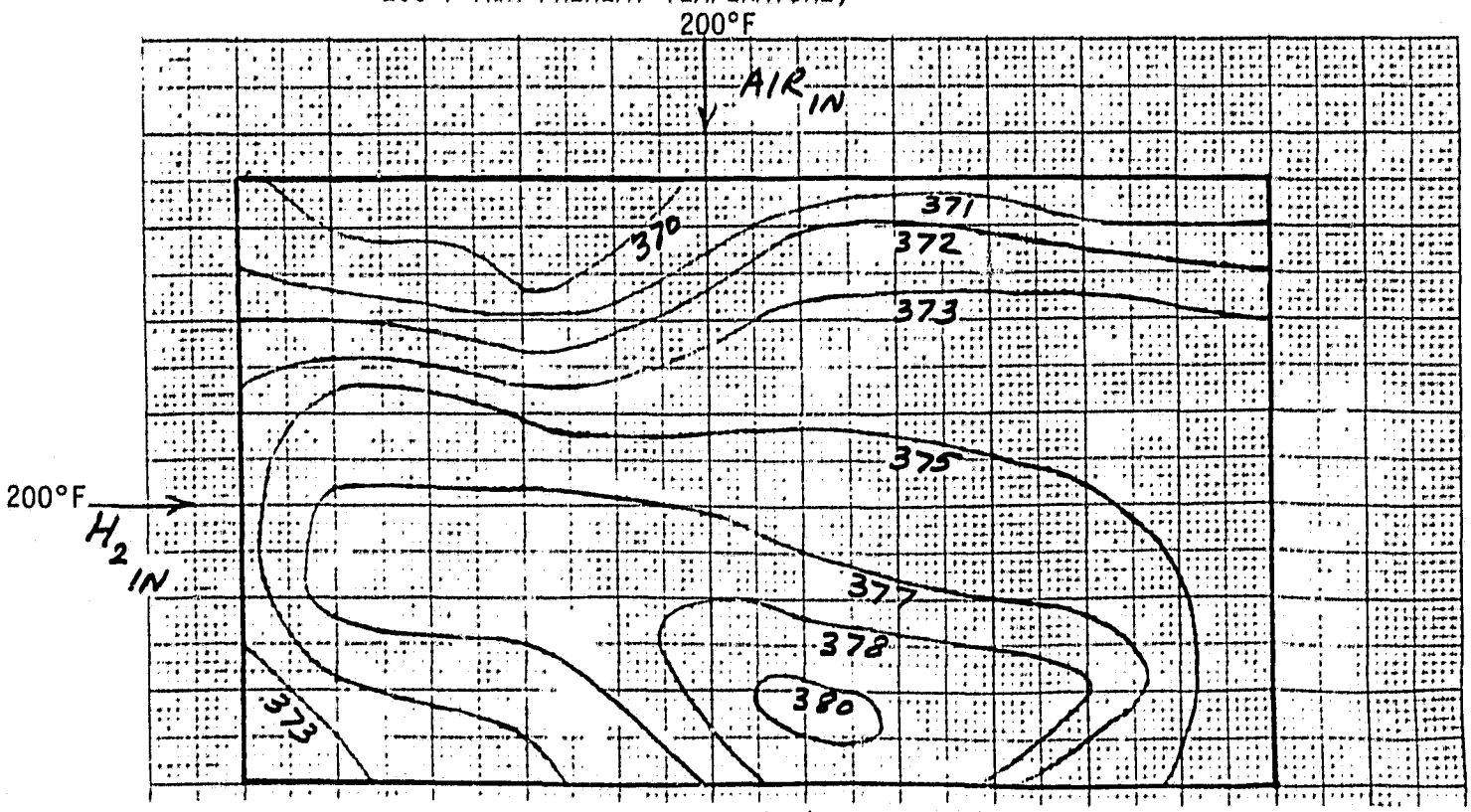

FIGURE 8 CELL TEMPERATURE PROFILE (°F) IN 24-CELL STACK WITH METALLIC COOLING PLATES

(ADJACENT TO COOLING PLATE, CELL NO. 12; 2.5x STOICH. AIR; 150 ASF; 200°F AIR PREHEAT TEMPERATURE)

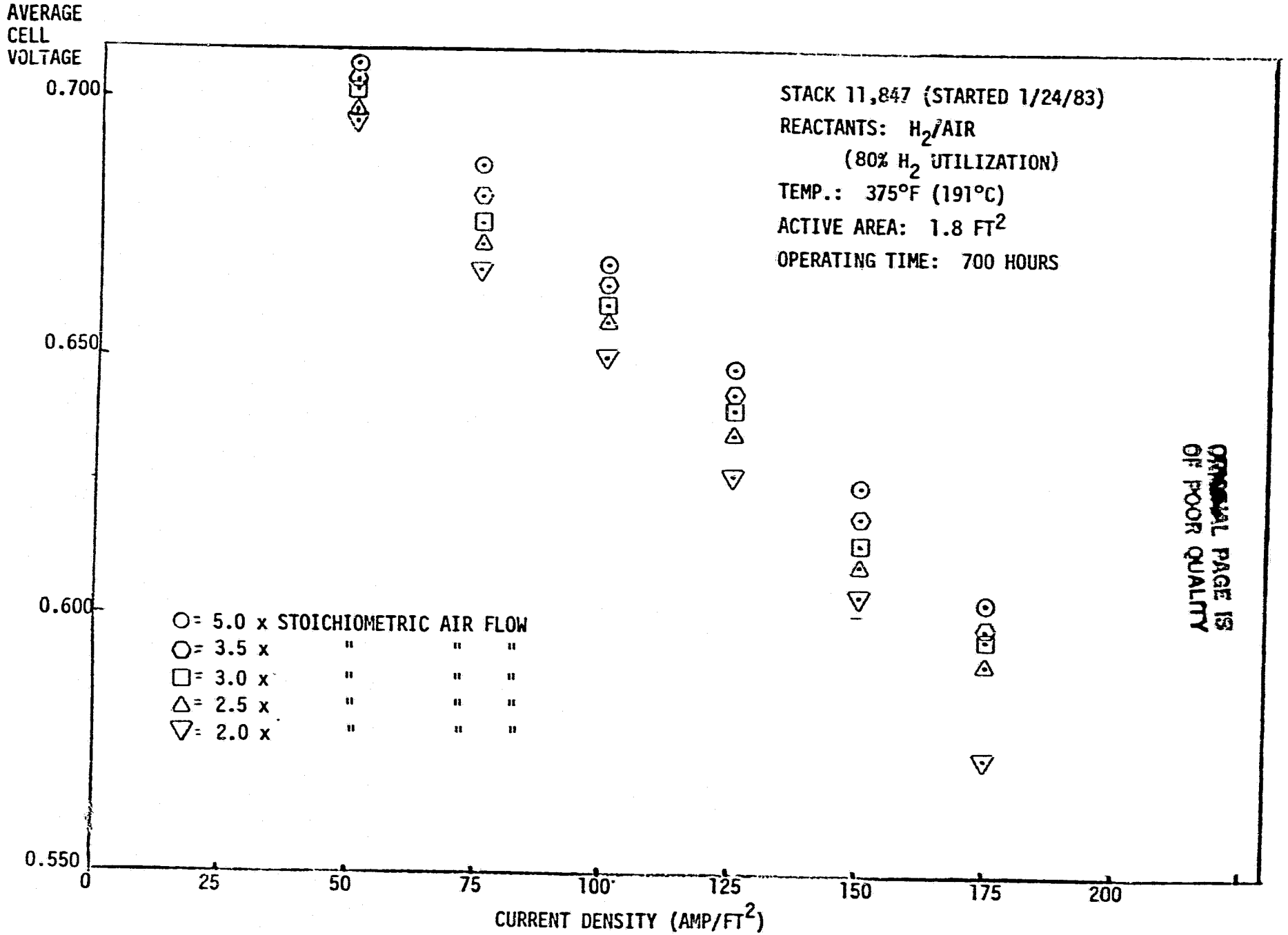

FIGURE 9 EFFECT OF AIR FLOW RATE ON AVERAGE CELL PERFORMANCE IN 24-CELL STACK (2 FT^2)

ENGELHARD

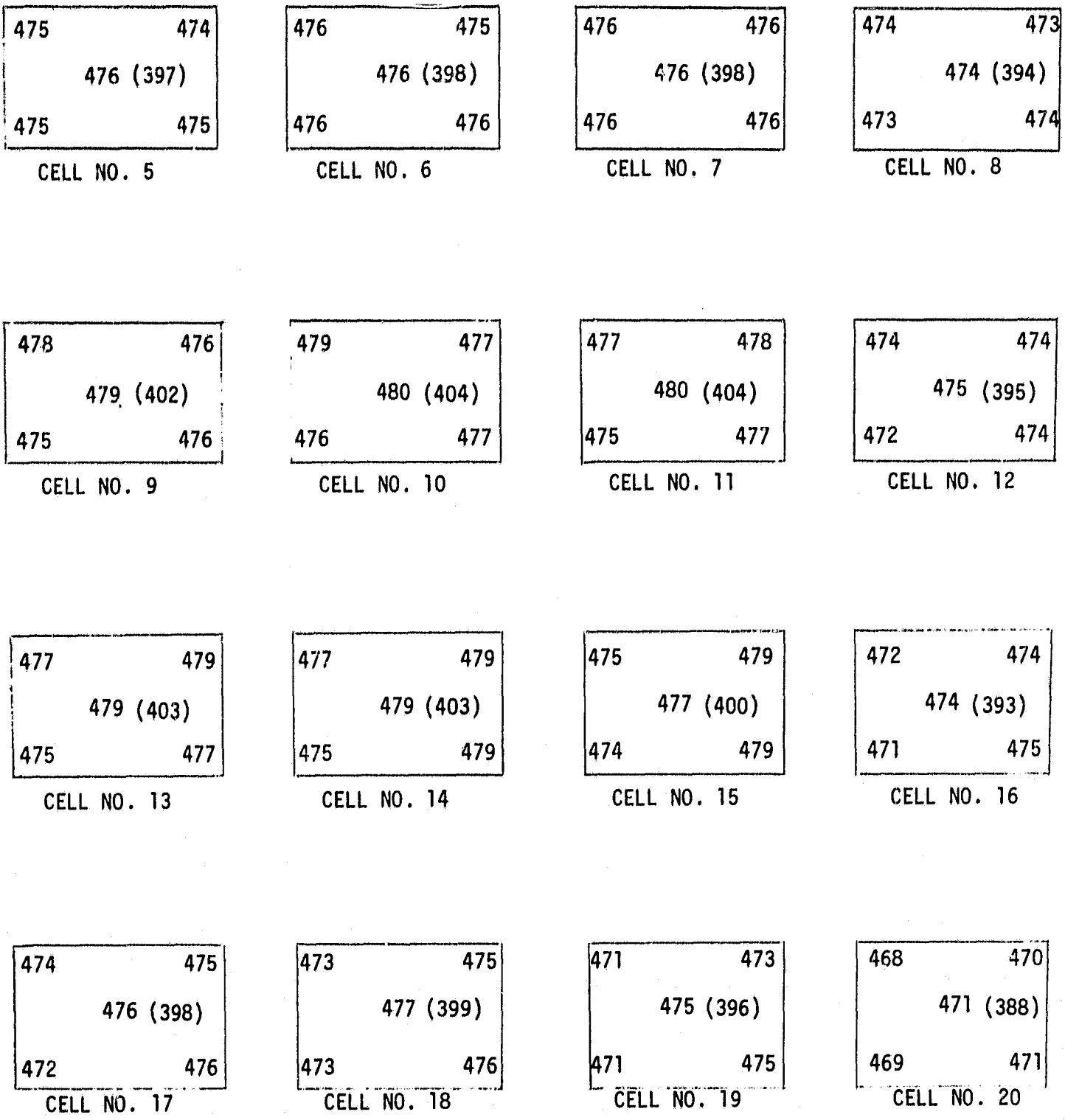

FIGURE 10 TEMPERATURE* PROFILES IN 24-CELL STACK WITH NON-METALLIC COOLING PLATES

* Temperatures in Kelvin (°F)

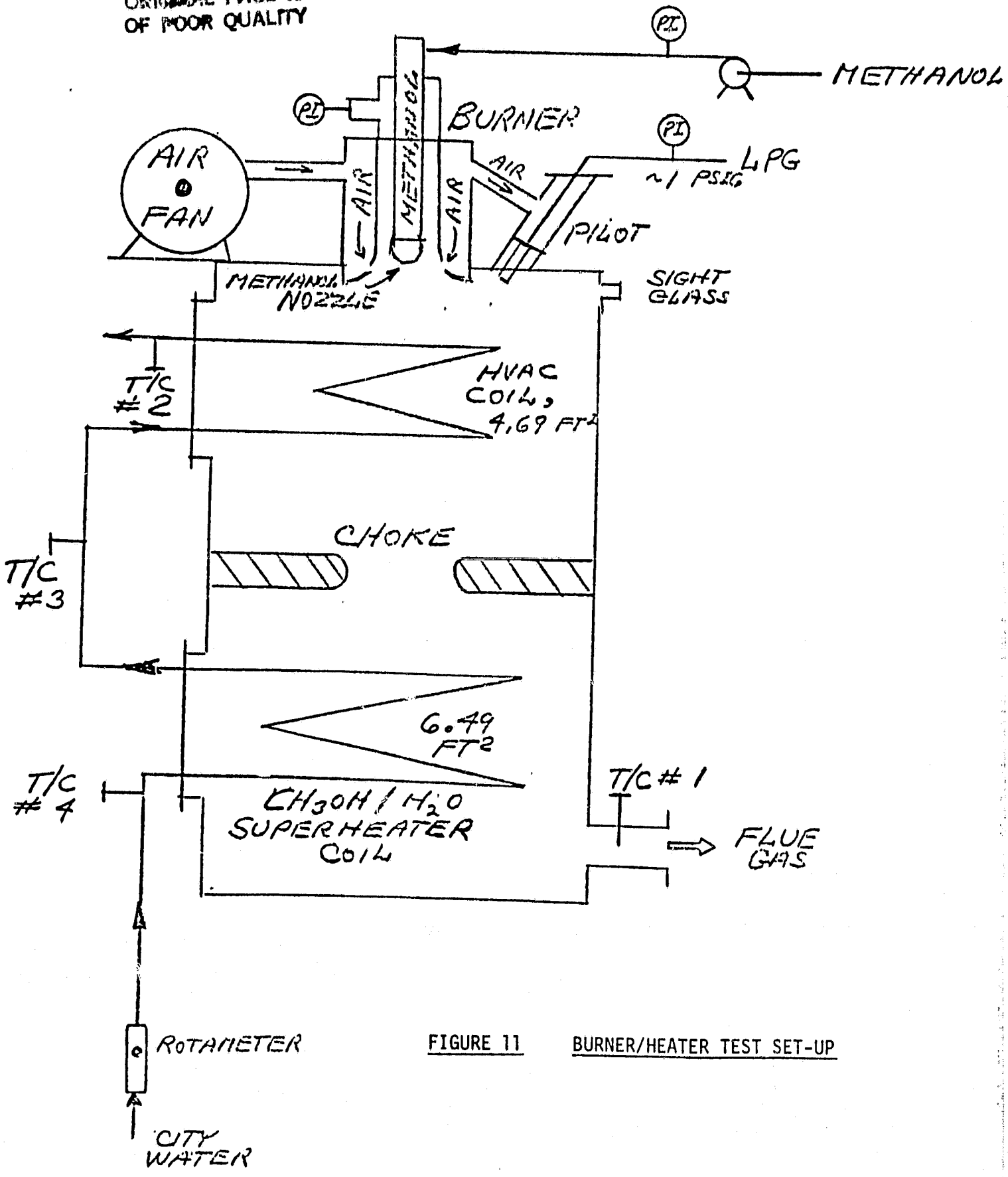

FIGURE 11 BURNER/HEATER TEST SET-UP

RMY
2/2/10

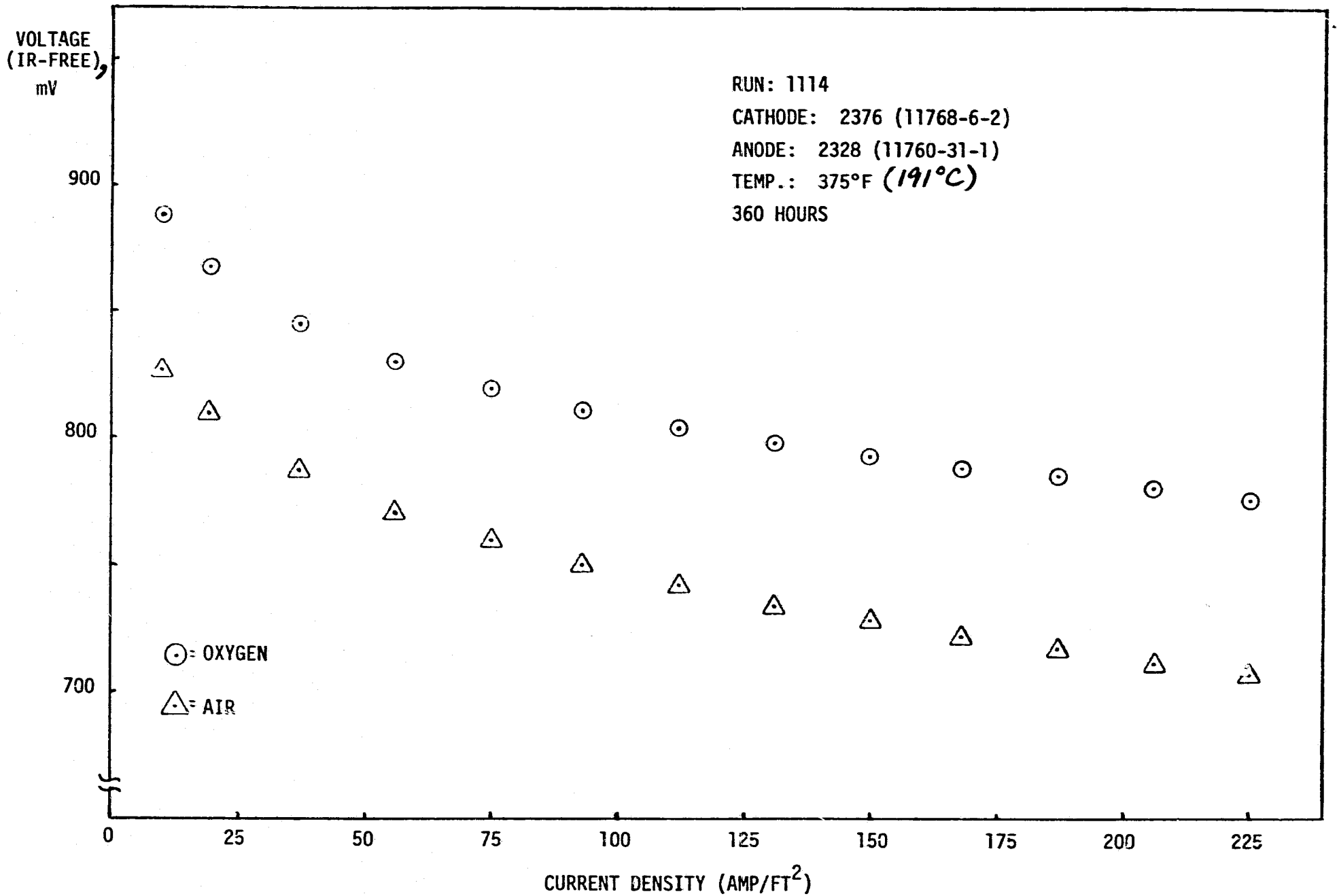

FIGURE 12 VOLTAGE (IR-FREE) VS. CURRENT DENSITY OF A SINGLE-CELL UTILIZING AN E-7 CATHODE CATALYST

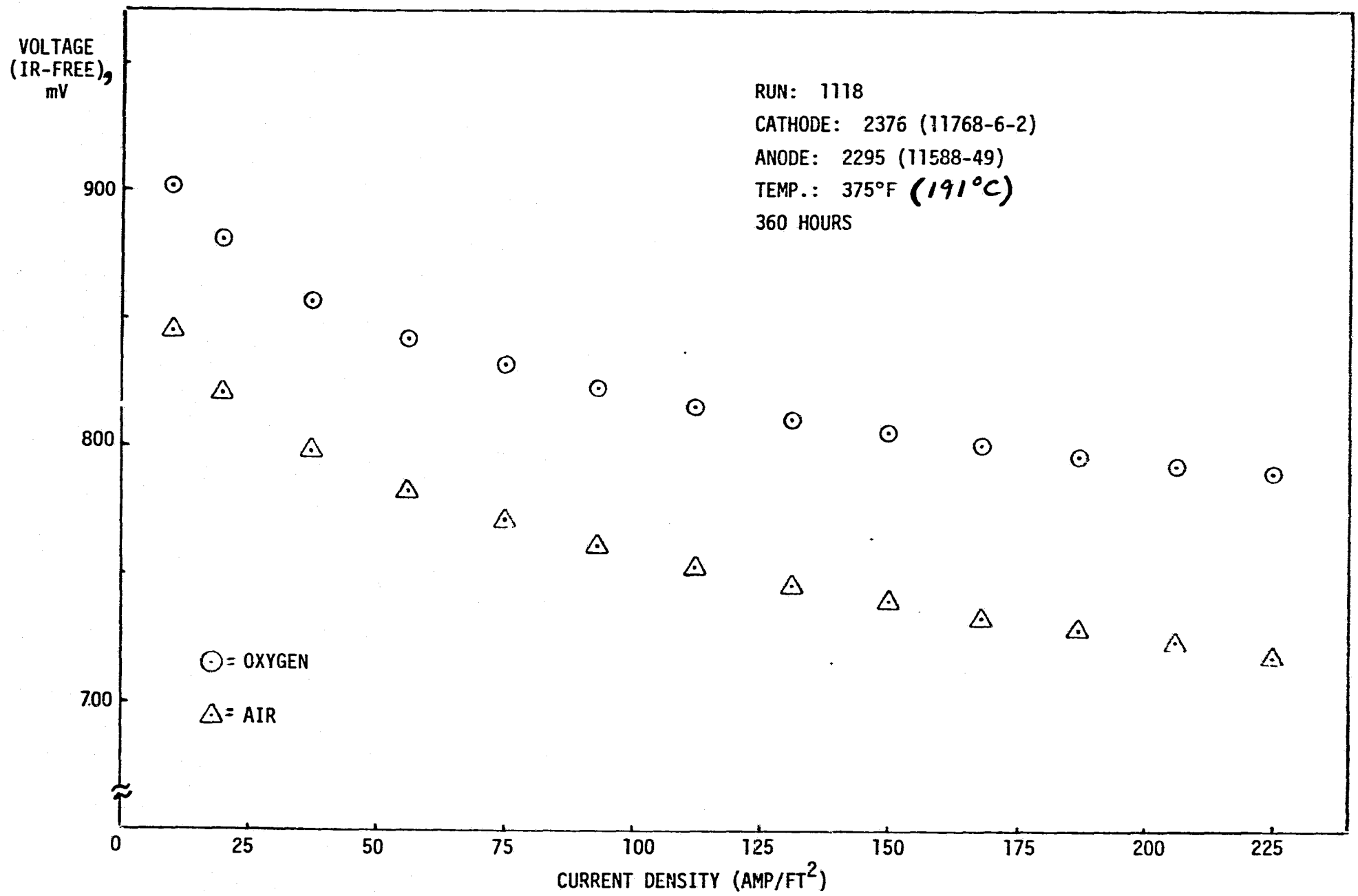

FIGURE 13 VOLTAGE (IR-FREE) VS. CURRENT DENSITY OF A SINGLE-CELL UTILIZING AN E-7 CATHODE CATALYST

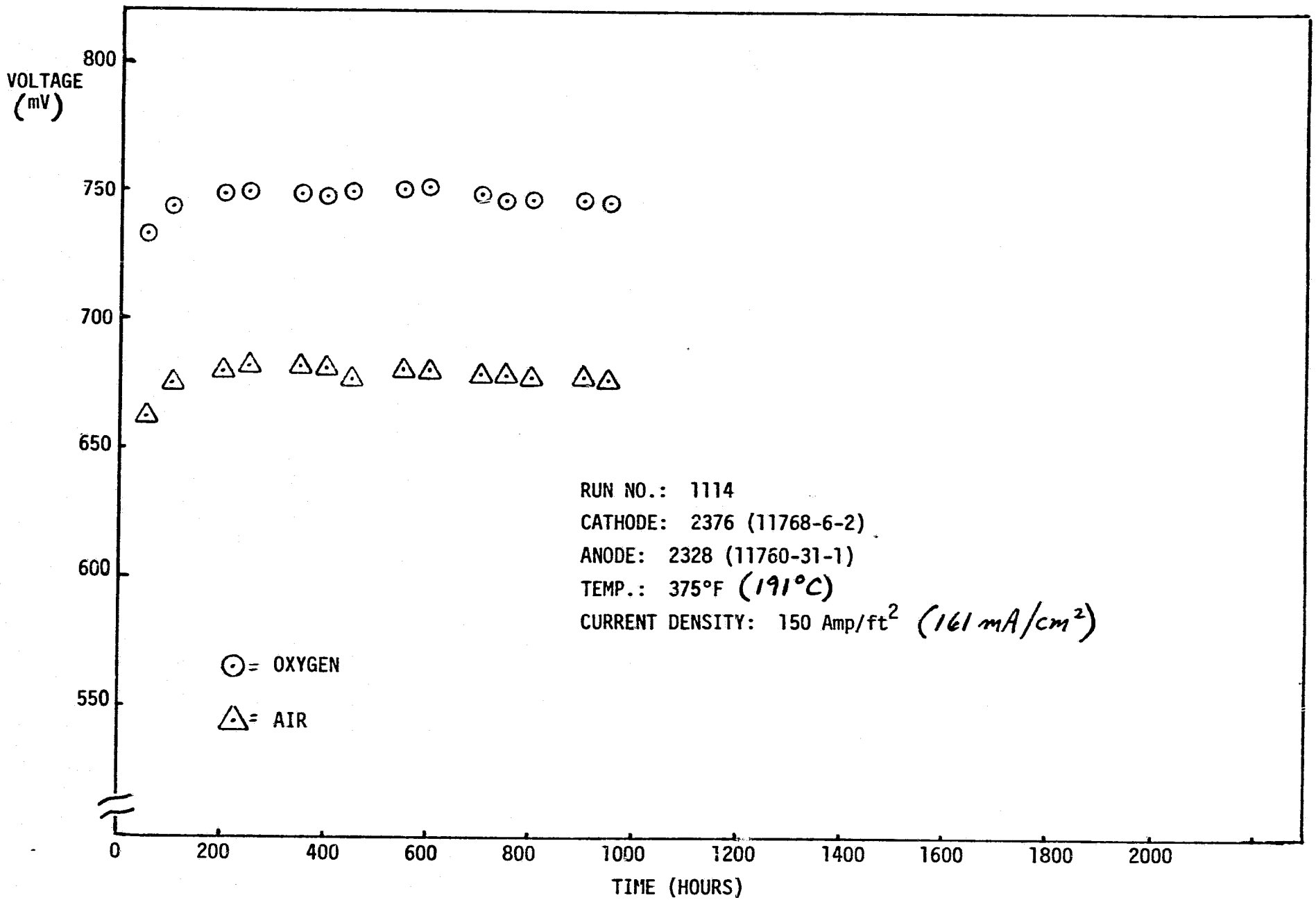

FIGURE 14 PERFORMANCE STABILITY OF A SINGLE-CELL UTILIZING AN E-7 CATHODE CATALYST

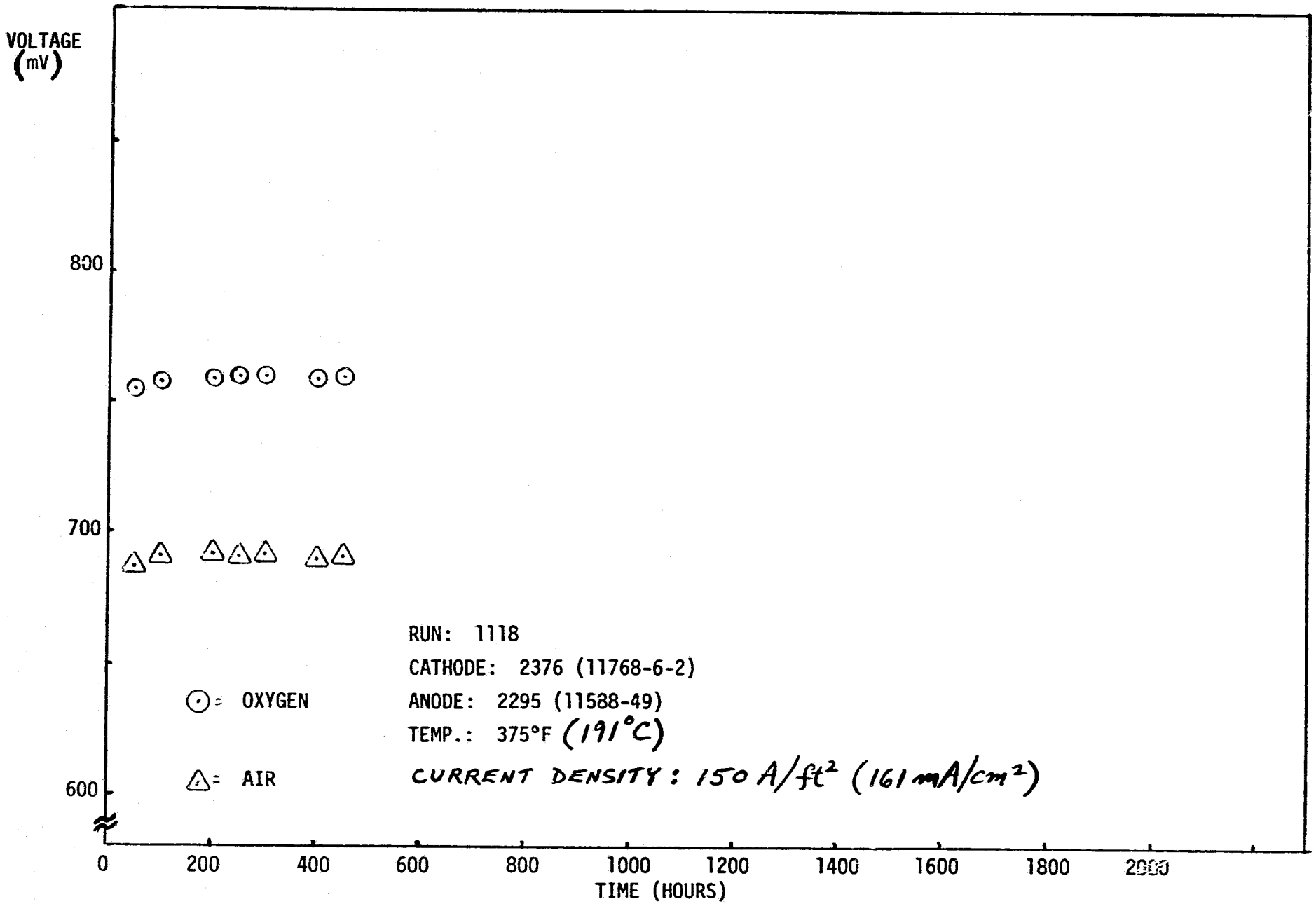

FIGURE 15 PERFORMANCE STABILITY OF A SINGLE-CELL UTILIZING AN E-7 CATHODE CATALYST

3/7/83

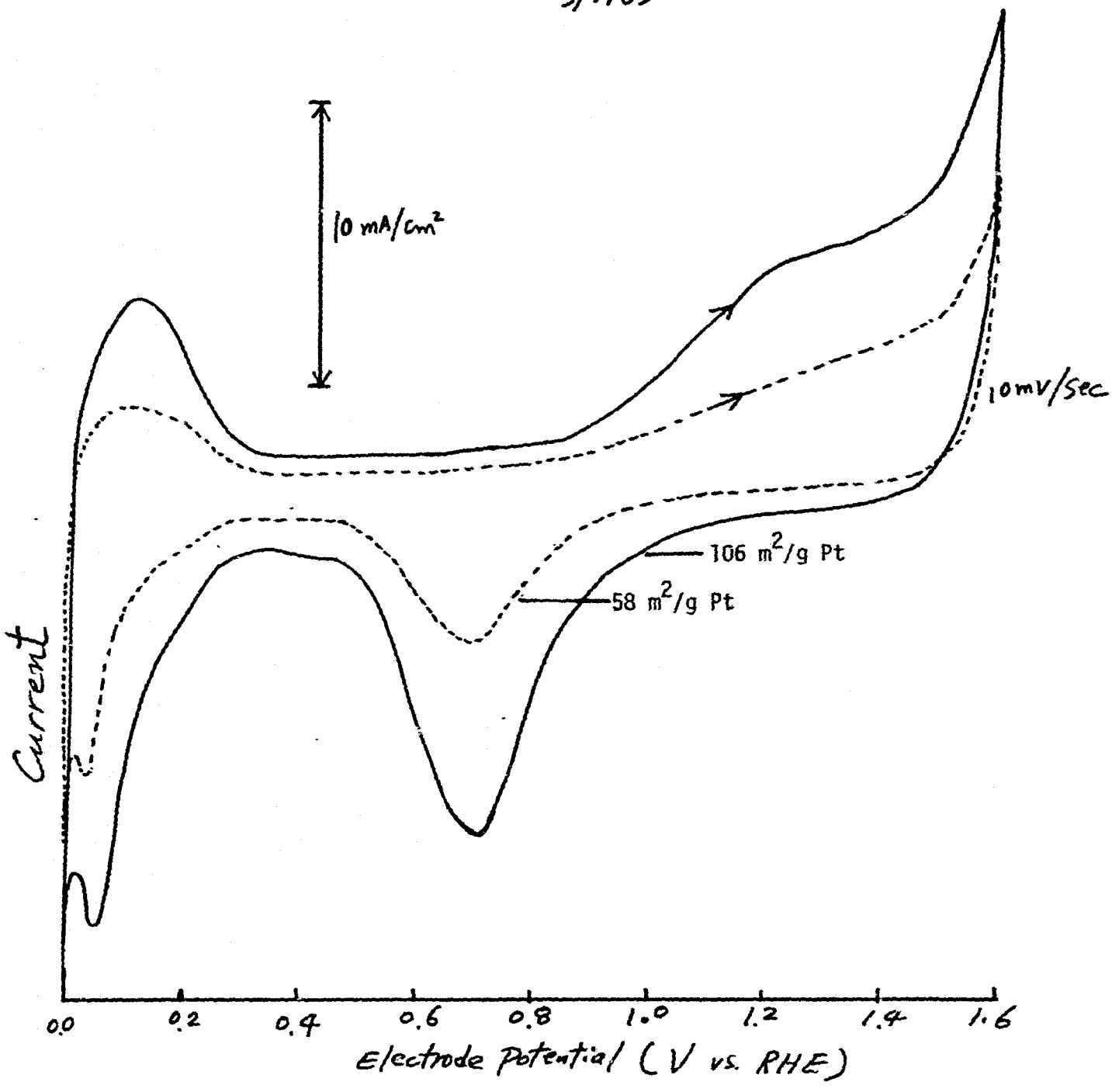

FIGURE 16 VOLTAMMOGRAMS OF FULLY-WETTED AND INCOMPLETELY-WETTED ELECTRODE SAMPLES IN 25% H_3PO_4 AT 25°C.

3/9/83

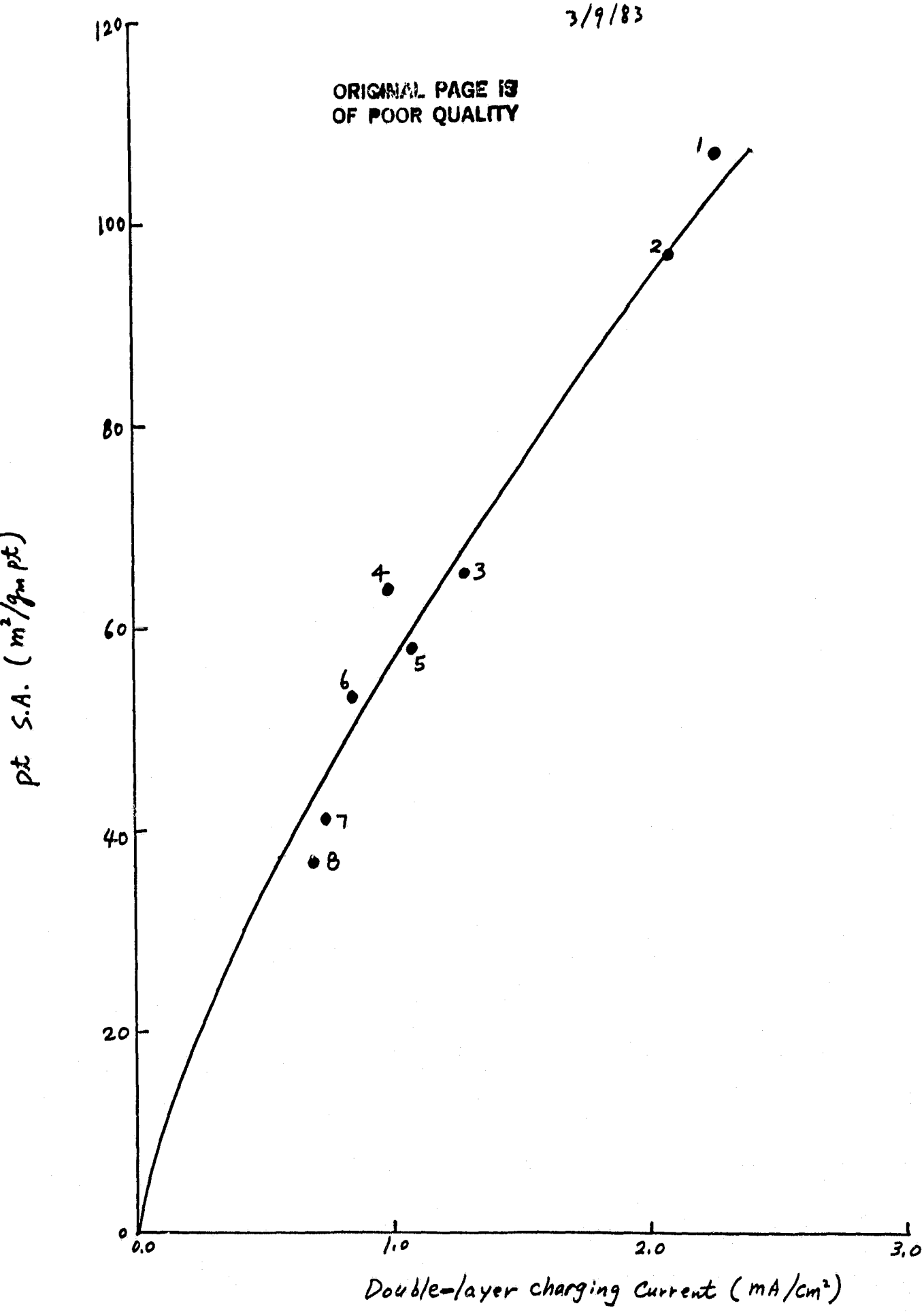

FIGURE 17 ELECTROCHEMICAL PLATINUM SURFACE-AREA AS A FUNCTION OF DOUBLE-LAYER CHARGING CURRENT

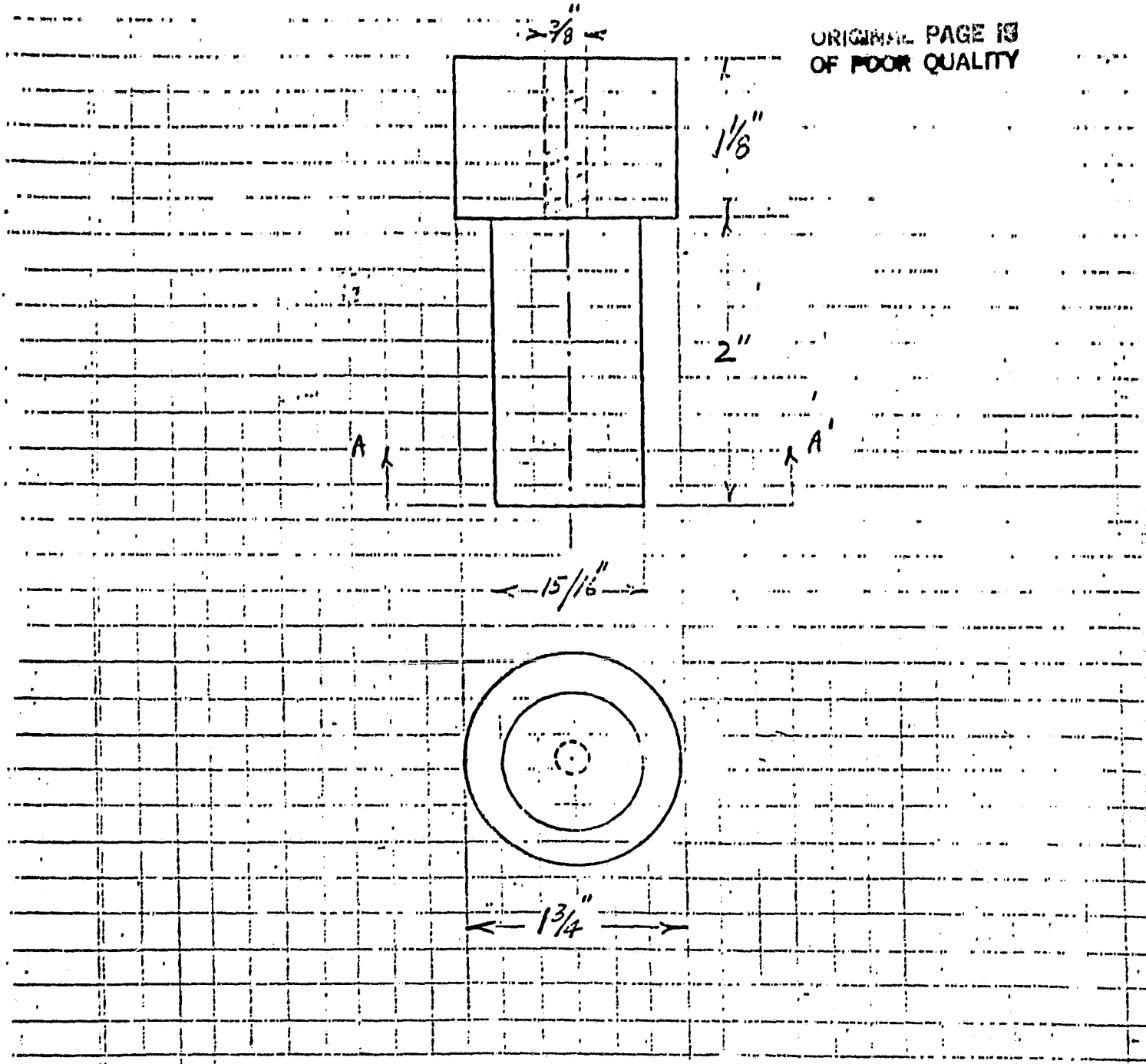

FIGURE 18 FIXTURE FOR CARBON PAPER SHEAR STRENGTH DETERMINATION

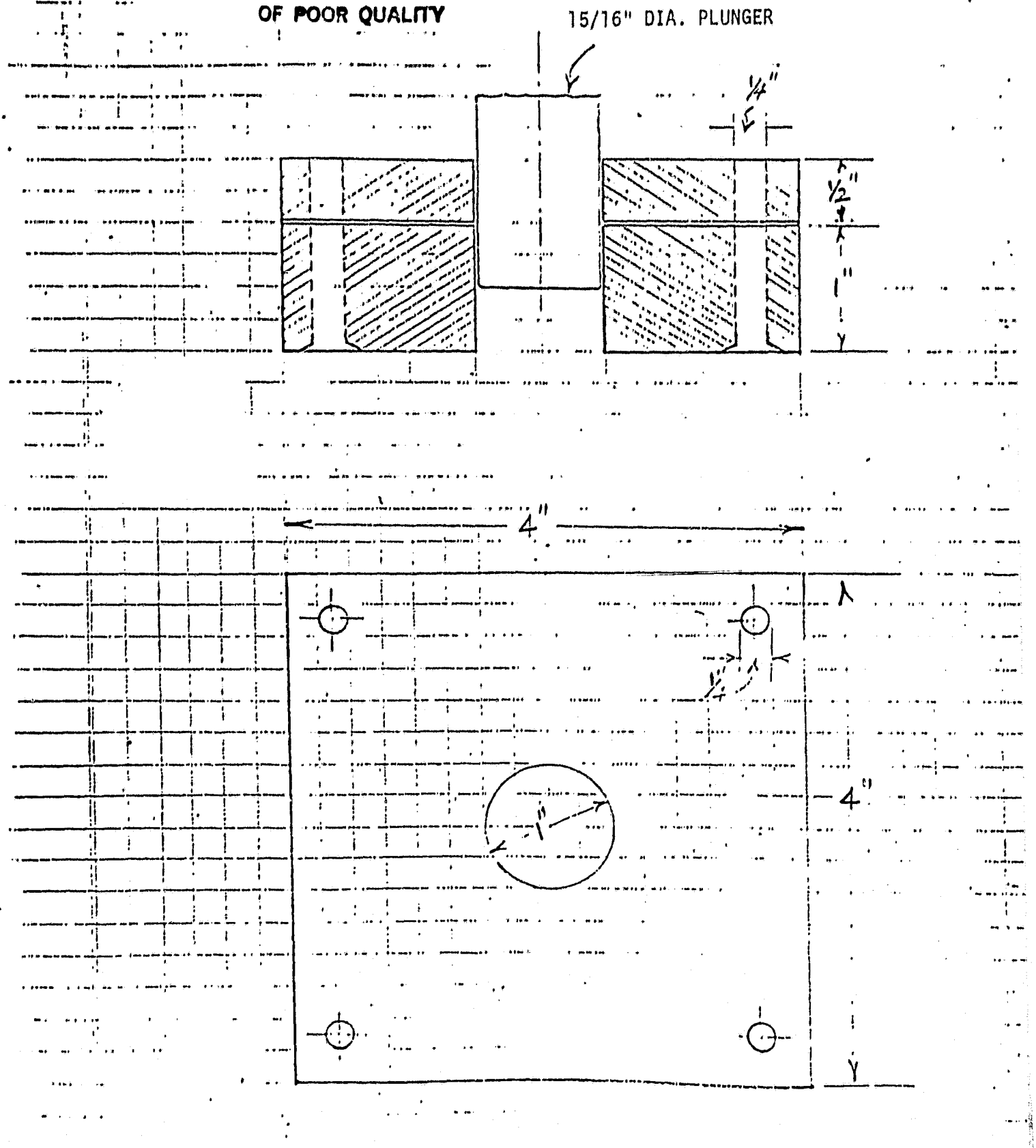

FIGURE 19 FIXTURE FOR CARBON PAPER SHEAR STRENGTH DETERMINATION

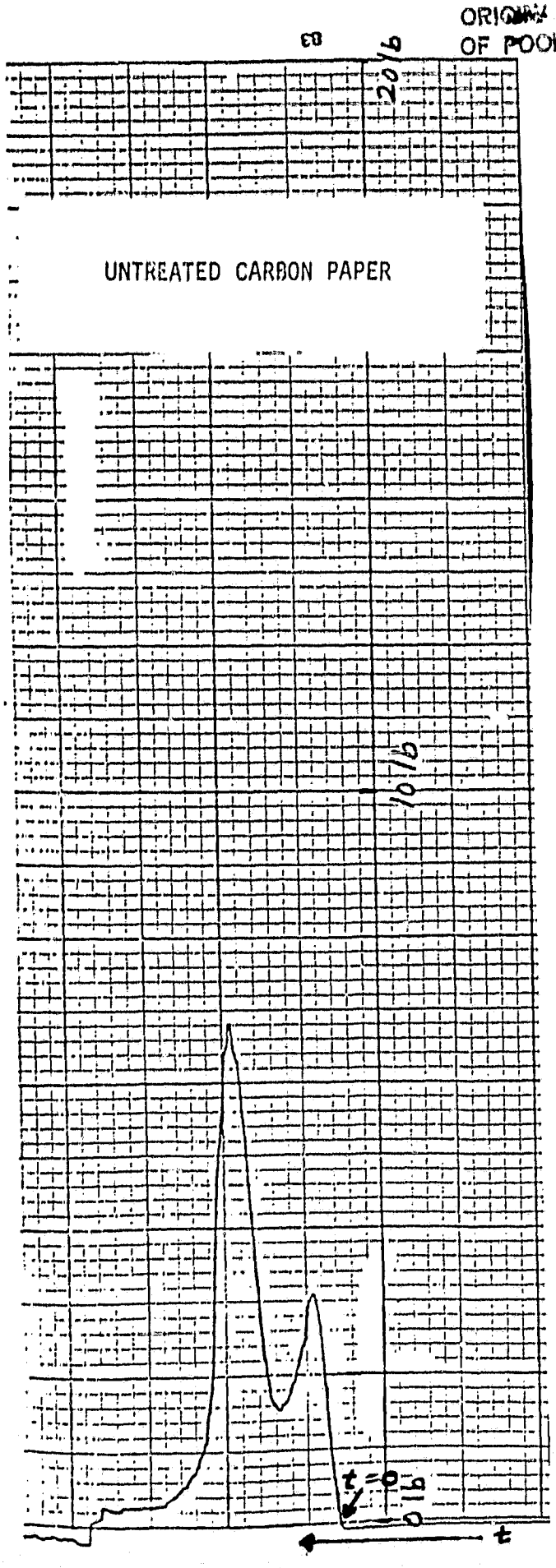

FIGURE 20 CARBON PAPER FAILURE TEST TRACE

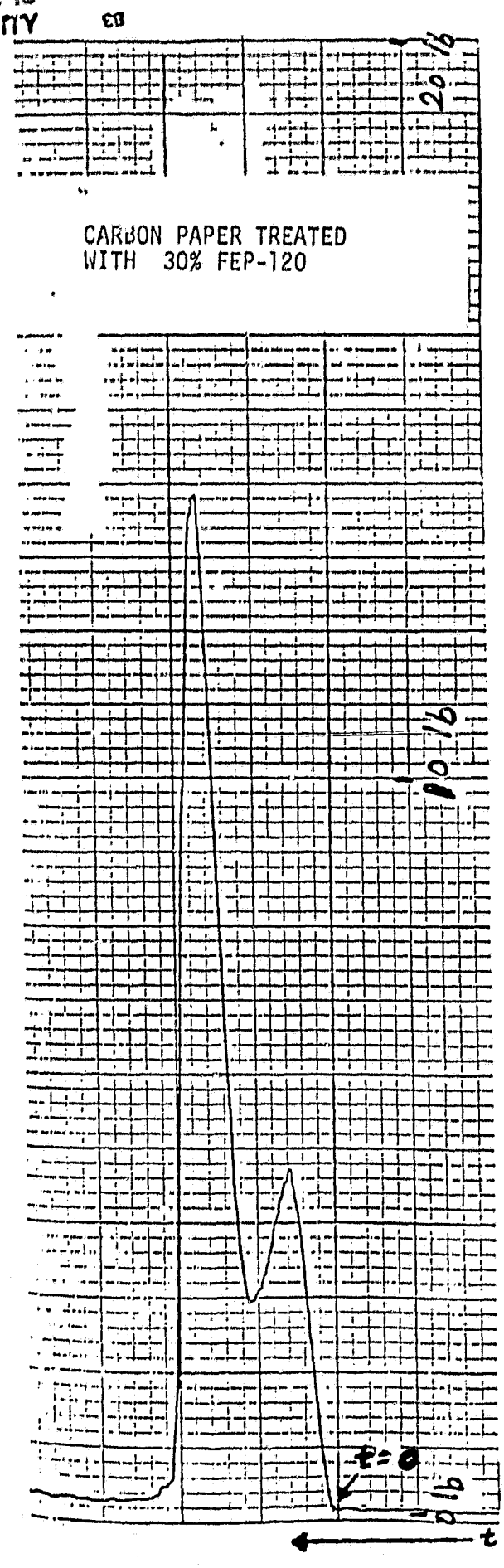

FIGURE 21 CARBON PAPER FAILURE TEST TRACE

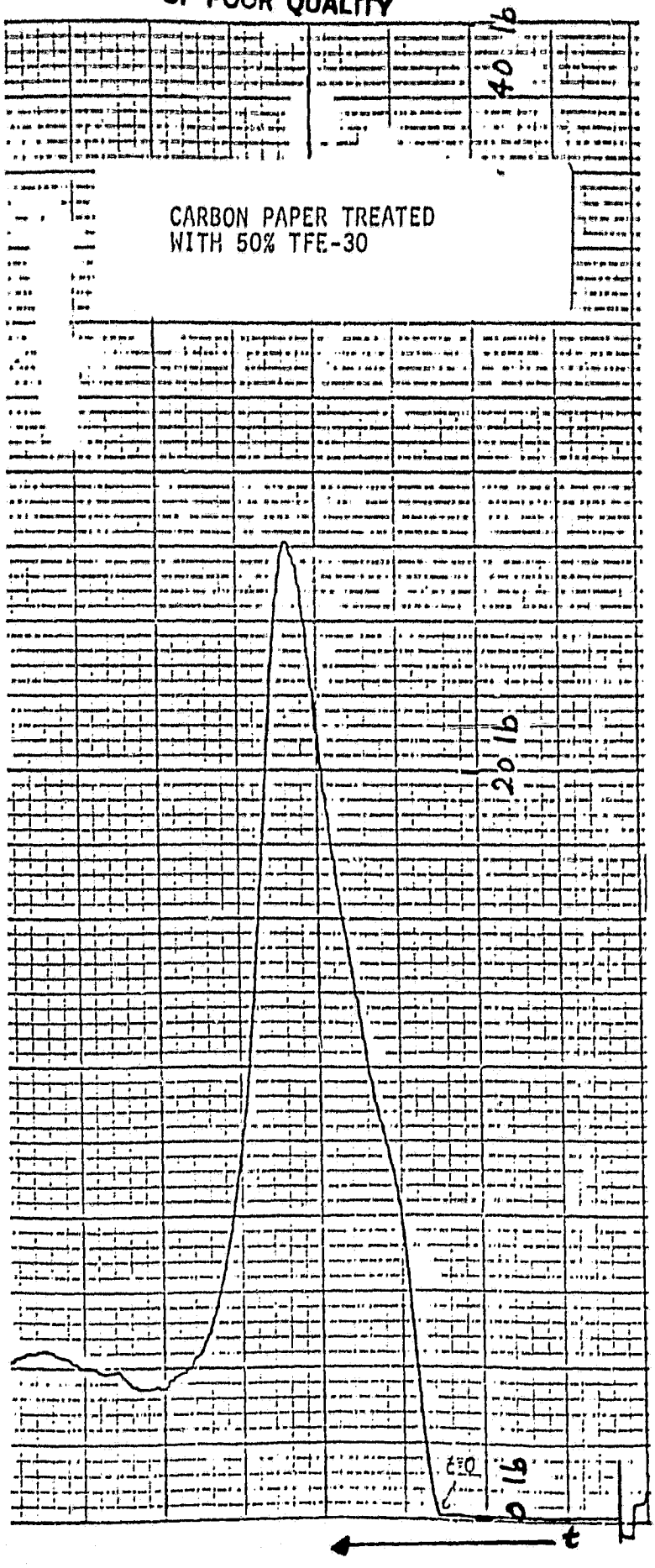

Figure 22 CARBON PAPER FAILURE TEST TRACE

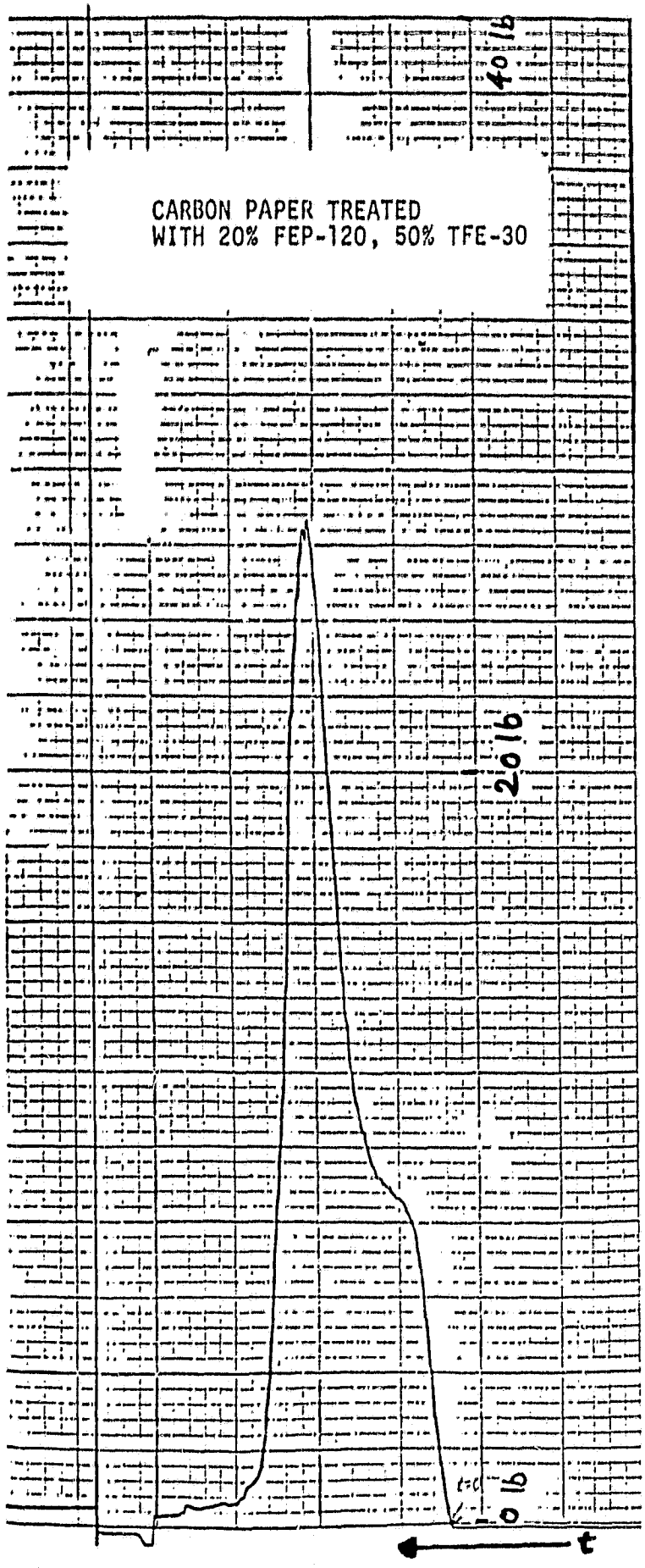

FIGURE 23 CARBON PAPER FAILURE TEST TRACE

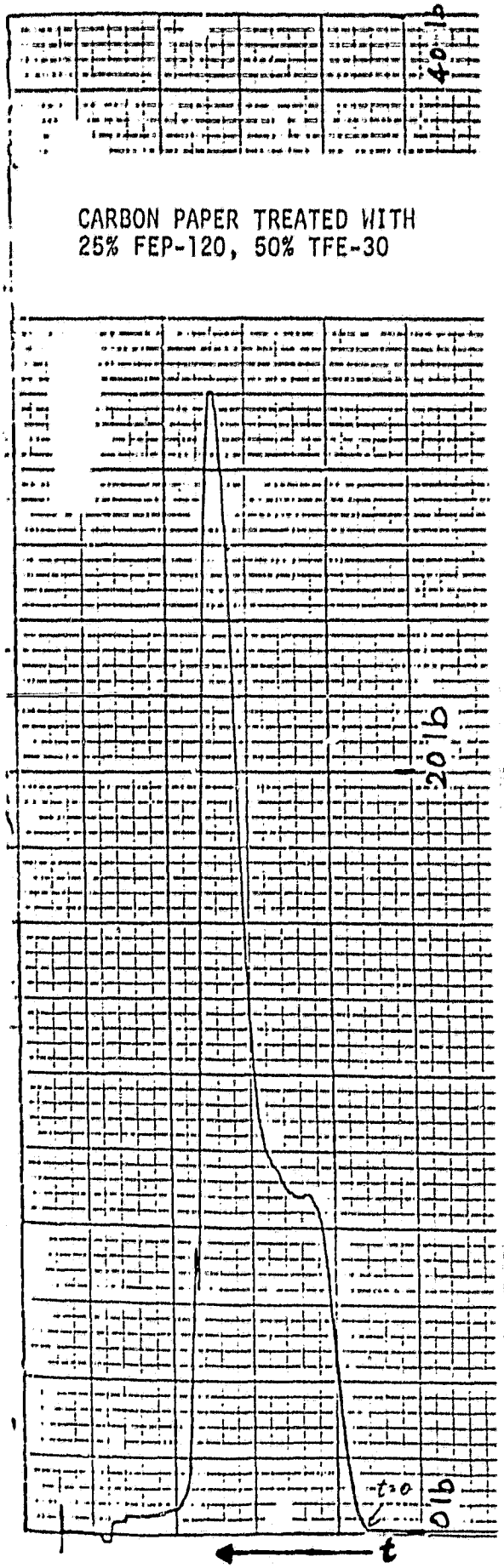

FIGURE 24 CARBON PAPER FAILURE TEST TRACE

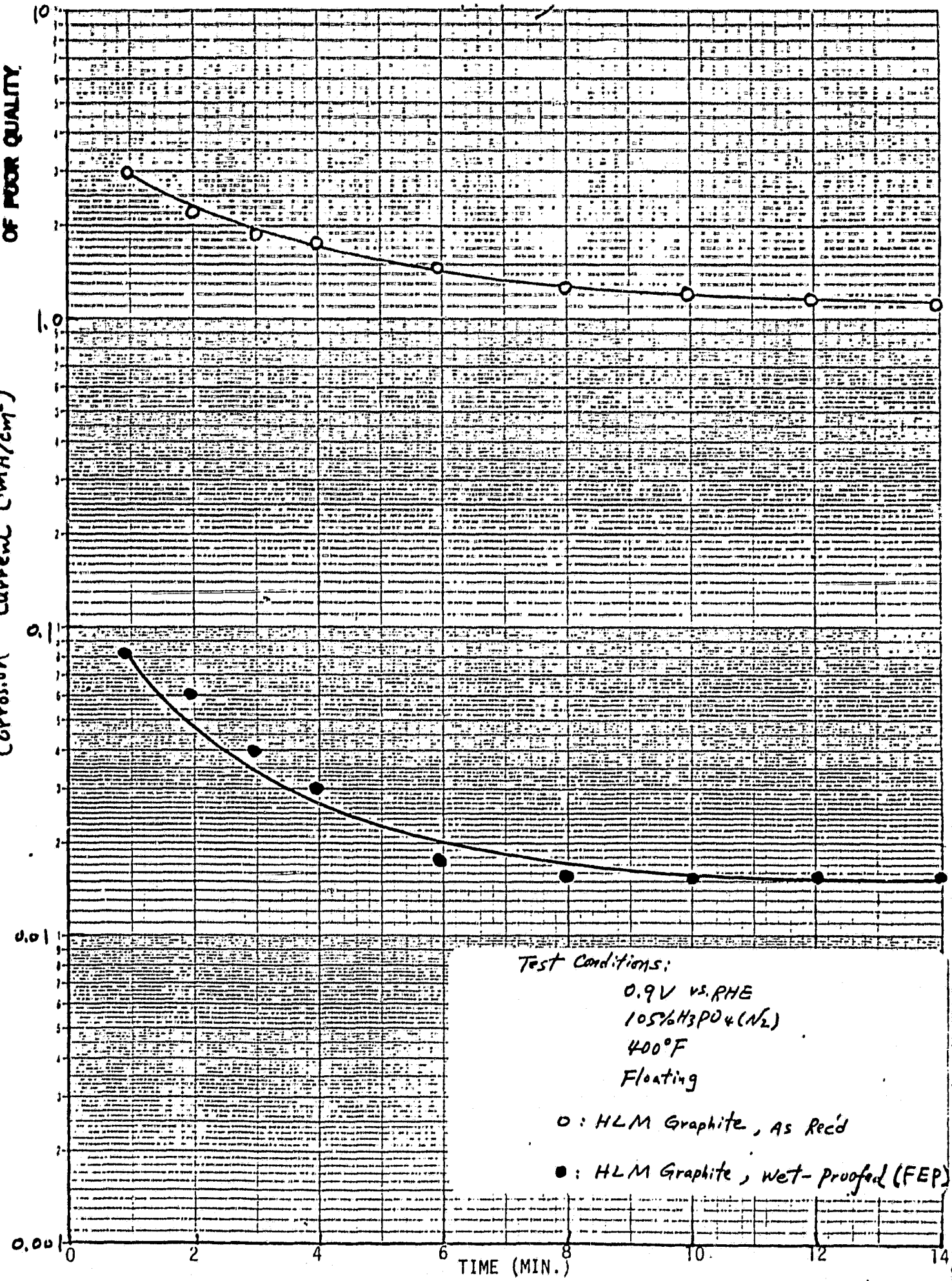

FIGURE 25 EFFECT OF WETPROOFING ON CORROSION OF HLM GRAPHITE